UNIVERSITY OF CALIFORNIA SAN DIEGO

Spatiotemporal Dynamics of Bacterial Colonies on Hard Agar

A Thesis submitted in partial satisfaction of the requirements
for the degree Master of Science

in

Bioengineering

by

Kinshuk Sahu

Committee in charge:

Professor Terence Hwa, Chair
Professor Bernhard Palsson, Co-Chair
Professor Bo Li
Professor Prashant Mali

2022

The Thesis of Kinshuk Sahu is approved, and it is acceptable in quality and form for publication on microfilm and electronically.

University of California San Diego

2022

DEDICATION

I would like to dedicate this thesis to my family, especially in loving memory of my grandfather, B.L Sahu, who unfortunately passed away on May 4th 2021 due to complications arising due to Covid-19. He was my biggest supporter and motivator, and I hope that I can make him proud in the years to come.

TABLE OF CONTENTS

LIST OF FIGURES

LIST OF SUPPLEMENTAL FILES

Supplementary Figure S1: Sahu_01_KmAcetate.png

Supplementary Figure S2: Sahu_02_GrowthGlucose.png

Supplementary Figure S3: Sahu_03_InitialDensity.png

Supplementary Figure S4: Sahu_04_CmPlates.png

Supplementary Figure S5: Sahu_05_ColonyDiameter.png

Supplementary Figure S6: Sahu_06_LactoseGradient.png

Supplementary Figure S7: Sahu_07_AcetateThin.png

Supplementary Video 1: Sahu_08_Colony3D.avi

ACKNOWLEDGEMENTS

Firstly, I would like to acknowledge Prof Terence Hwa for giving me the opportunity to take part in this wonderful project and advising me throughout my stay in his lab. I would also like to thank him for guiding me towards a better thinker and researcher, and also for all his support, especially during the tough initial times of the pandemic.

I would like to thank Tolga Caglar, for having patience and helping me guide during my initial experimental days in the lab, and also when I joined the colony project. I would like to thank Harish Kannan for the countless discussions about the colony project, and helping me to better understand the computational side of the project and for sharing his computational and experimental data with me. I would also like to acknowledge the rest of the faculty members involved in the Colony Project- Prof Bo Li, Prof Paul Sun and Prof Jiajia Dong for sharing their insights and for the constant productive discussions we had throughout my time in this project.

I would also like to express my gratitude to the Hwa lab members for maintaining a fun and supportive atmosphere in the lab and for always being ready to answer my questions. First of all, I would like to thank Zhongge Zhang in helping in the creation of all the *E. coli* strains used in this work, often at very short notice and helping me understand about molecular biological techniques in general. I would especially like to thank Jacob Robertson for all his guidance and support with experiments involving the confocal microscope and with image processing. I would also like to thank Gabriel Manzanarez, Ghita Guessous, Kapil Amarnath, Brian Taylor, Chenhao Wu, Rohan Balakrishnan and Hiroyuki Okano for sharing their experimental protocols whenever I needed them or having rich discussions about science or about the cross-feeding project.

I would like to thank all the faculty members- Prof Terence Hwa, Prof Bo Li, Prof Bernhard Palsson and Prof Prashant Mali for agreeing to be a part of my thesis defense committee. Thanks a lot, to Prof Bernhard Palsson for agreeing to co-chair my committee along with Prof Terence Hwa.

Lastly, I would like to thank all my family members and friends for believing in me and for their moral support throughout my academic career.

Chapter 1, in part, is in part is currently being prepared for submission for publication of the material with Kannan, Harish.; Caglar, Tolga; Ge, Daotong, Dong, Jiajia; Sun, Paul; Zhang, Zhongge; Li, Bo and Hwa, Terence. The thesis author was a primary researcher and author of this material.

Chapter 2, contains unpublished material coauthored with Kannan, Harish; Caglar, Tolga; Segota Igor; Zhang, Zhongge; Sun, Paul; Li, Bo and Hwa, Terence. The thesis author was a primary author of this chapter.

ABSTRACT OF THE THESIS

Spatiotemporal Dynamics of Bacterial Colonies on Hard Agar

by

Kinshuk Shau

Master of Science in Bioengineering

University of California San Diego, 2022

Professor Terence Hwa, Chair

Professor Bernhard Palsson, Co-Chair

Biofilms are ubiquitous in nature, having dense spatio-temporal structures containing various types of social interactions between different microbial communities. In this study, we use colony growth of E. *coli* cells on hard agar as a model system for biofilm dynamics. Employing a combination of experimental and modeling techniques, we first quantify the growth characteristics of an *E. coli* colony starting from a single cell. The agent-based simulations capture spatio-temporal dynamics of important metabolites, with the gradients of these metabolites suggesting physiological differentiation occurring across the colony. To

further mimic natural biofilms, we then implemented trophic interactions between a pair of *E. coli* strains. Confocal microscopy images of a producer-consumer cross-feeding colony show the formation of unique flower-like patterns with the consumer enveloping the producer at the colony frontier. Experimental measurements reveal that the consumer can compensate for its lower growth rate, compared to the producer, with a lower Monod constant, allowing it to coexist with the producer in the initial phase. We find that as colony growth progresses, the consumer, despite having a slower radial expansion rate on one nutrient, can keep up with the producer at the frontier by employing a simultaneous nutrient utilization strategy as opposed to hierarchical for the producer. In the final regime of colony growth, while the producer slows down because of nutrient depletion, the consumer continues to grow, eventually forming the patterns. In conclusion, this work demonstrates the role of physiological diversity and community interactions on bacterial colony growth.

CHAPTER 1: Dynamics of Single Strain *E. coli* Colonies

1.1 Introduction

Bacterial communities are known to exist in the environment in the form of biofilms, wherein using the secretion of biopolymer substances such as extracellular polymeric substances (EPS), they attach to surfaces and form dense spatio-temporal heterogenous structures [1]. These structures are influenced by a vast array of factors including colony growth, mechanical interactions, motility, signaling pathways and these diverse interrelated components make it quite a difficult system to study [2]. In recent years, many studies have focused their attention instead on a toned-down version of biofilms- colony growth of non-motile, non-EPS producing bacteria on hard agar [3][4]. Insights gained from the factors influencing colony growth on bacteria on hard agar can play crucial roles in deciphering the ubiquitous and complex biofilm interactions found the wild.

The earliest quantitative studies of this simplified system of bacteria growing on agar date back to radial colony measurements made by Pirt in 1967[5], and followed up by others [6] determining other parameters like height, the variability of these parameters between different microbial species and on environmental conditions such as nutrient availability, agar concentration, mode of growth etc. Despite the multitude of these studies, our quantitative understanding was still lacking about the factors which controlled the growth of the colony. An earlier version of our study-Warren et al, 2019[3], along with numerous other works over the past decade [4][7][8] have employed biophysical computational models to narrow this knowledge gap. Our particular study involved using a 3D agent-based simulation model incorporating the effects of nutrient diffusion, cell-cell and cell-agar interactions and cell level model of surface tension, and demonstrated that while nutrient penetration affected the colony height, radial expansion was limited by the mechanical interactions of the colony with the agar.

Our earlier study was mainly concerned with the linear increase in radial and vertical expansion speeds during the first 24 hours after seeding the colony. Although we had observed that while radial expansion speed remained constant throughout this period, a slowdown occurred in the rate of increase of colony height beginning around 24 hours. In this study, we focus our attention on elucidating the main factors causing this slowdown, and build upon our original agent-based model by including major metabolic processes that can influence colony growth- for example, nutrient consumption, oxygen diffusion, anaerobic growth and fermentation, and nutrient consumption for maintenance in absence of growth.

1.2 Material and Methods

1.2.1 Strain and Batch culture conditions

The parent strain used in our experiments is EQ59, as reported in Warren et al, 2019[3]. The strain is constructed on NCM 3722 background with a deletion in the *motA* gene to remove motility and having constitutive chromosomal GFP expression. For constructing EQ59 Δ*aceA*, JW3975 (BW25113 Δ*aceA*: kan, Keio collection [9]) served as a donor for P1 transduction with E. coli K-12 NCM 3722, yielding the strain NQ561. NQ561(NCM 3722 Δ*aceA*: kan) was then used as a donor for P1 transduction with the parent EQ59 strain.

`Phosphate buffered saline (PBS) was used as the buffer for the minimal growth media, with the addition of glucose as the carbon source and ammonium chloride as the nitrogen source. Unless specified, the final phosphate concentration of the buffer was kept at 112mM, while the glucose and ammonium chloride concentrations were kept at 20mM and 10mM respectively. On low buffer conditions, the phosphate concentrations were adjusted accordingly and appropriate changes were made in the salt concentration to keep the osmolarity fixed at 0.4M. For batch culture growth measurements, a seed culture in LB media was started from a single colony picked from an LB plate. After the culture becomes saturated

around 4-5 hours, the samples were washed and resuspended in PBS without carbon or nitrogen sources. The cultures were then diluted and transferred into minimal medium at low OD (~$0.5\ x\ 10^{-5}$) to ensure that it would be in the exponential growing phase the next day (around OD 0.5). The inoculum was transferred on the next day from the overnight minimal media tubes into fresh culture such that the OD was in the range of 0.02-0.05. Growth rate measurements, if done, were using a UV-Vis spectrophotometer in the OD range from 0.04-0.5.

1.2.2 Preparation of minimal media agar plates and plate inoculation for colony growth

The agar plates were prepared on the same day as the seed culture with final agar concentration being kept at 1.5% w/v. 16ml of molten agar with minimal media was poured onto petri plates of dimensions 60 mm x 15mm, resulting in an agar depth of around 8 mm. The plates were allowed to solidify in an open flame around the bench for about 10-15 minutes, and were then dried in a PCR hood for another 10 minutes and stored at 4^{o}C for inoculation on the next day.

When the cultures were around an OD of around 0.25-0.3, 100 µL of the culture was taken and was serially diluted 10^6 times, and 100uL was poured using a micropipette onto the pre warmed agar plates, and the inoculum was mixed uniformly onto the plate using glass beads. The dilution was done such that there would be around 5-10 colonies in the final plate, which for the plate size used corresponds to average colony spacing of around 1 cm radially till encountering another colony. After mixing, the plates were allowed to dry in the PCR hood for around 10 minutes and then wrapped with parafilm and stored in the 37°C incubator until being taken out the next day onwards periodically for colony growth measurements using confocal microscopy.

To allow for continuous colony growth measurements, multiple (5-6) plates were prepared on the same day separated by around 2 hours between inoculation times. The plates were sequentially scanned around every 12 hours with each confocal scan taking between 3-35 minutes depending upon the stage of

colony growth. This staggered imaging strategy could be employed since the measurements were quite reproducible between different plates and colony to colony as described in Warren et al, 2019[3].

1.2.3 Microscopy and Image Processing

Colonies were imaged at the appropriate times using a Leica TCS SP8 inverted confocal microscope enclosed in a 37^{o}C temperature enclosure. Parafilm was carefully removed and the colonies were placed onto the stage facing the 10x/0.3 objective. The excitation of the laser was set at 488nm for GFP fluorescence and a HyD SP GaAsP detector was used with the emission spectrum set in the range from 495 to 545 nm. Since the colonies occupy a large space, individual parts were imaged using a square tilescan grid and the final image was stitched together using a custom Python script.

After stitching the merged image, the script was used to calculate the radius and the height of the colony. The radius is obtained by going through all the z stacks images which have been processed through a Gaussian blur and thresholded. Using the smallest enclosing circle library by Project Nayuki, we then find the radius of the circle enclosing points whose pixel intensities are above a threshold. The surface is set to the point where the radius is maximum and the height of the colony is then calculated. This script also gives information about the radius of the colony at a particular height, which was used to generate the colony profiles. Plotting of the radius, height and profiles across time as the colony grows were done using a custom MATLAB Script.

1.2.4 Agent based model

Following our agent-based model from our earlier study [3], we model individual cells as a spherocylinder growing at a certain rate with individual cells adding a certain fixed length to its birth size and then undergoing division [10]. Mechanical interactions like forces and torque are implemented based on different types of interactions-

i) cell- cell interactions, arising when cells are in physical contact

ii) cell-agar interactions, for cells in contact with the agar surface

iii) cell-fluid interactions, cells interacting with surrounding fluid and experiences a viscous drag

iv) surface tension, a cell level model of surface tension with imbalances between surface tension and friction resulting in verticalization of cells due to "buckling"

In Warren et al, 2019 [3], just a single nutrient source was used to describe the growth of cells, and the authors had implemented a reaction diffusion model of nutrient dynamics and Dirichlet boundary conditions to fix the agar concentrations at the edge of the agar region. Since this study concerns with the transition and slowdown in the linear increase of height for colony growth beyond 24 hours, we expect oxygen limitation and anaerobic byproduct accumulation like acetate to play a role, and thus modelling the colony just with aerobic growth on a single carbon source is inadequate. An extended model has been implemented describing different growth modes of the colony under aerobic and anaerobic conditions, and as a byproduct of anaerobic metabolism, excretion of molecules like acetate which can diffuse through the colony. We also have added maintenance requirements for individual cells, as in if the nutrient is lower than a threshold quantity, the cell does not grow but uses the energy derived from these carbon sources for maintenance. One more modification that has been made is to reduce the simulation to (1+1) dimensions instead of (2+1) so that the computational solver is more efficient.

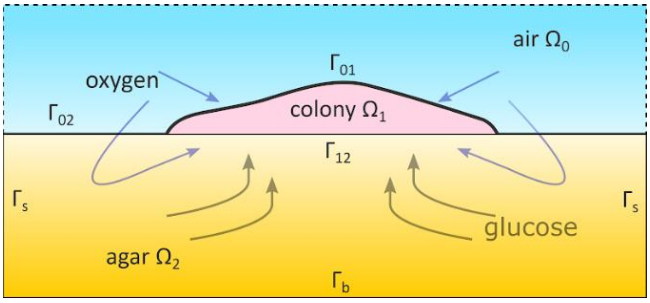

Figure 1: The geometry of the agent-based model of a colony growing on hard agar. The computational box is a two-dimensional rectangular region. It is divided into three parts: the air region Ω_0, the colony region Ω_1 that expands with time, and the fixed agar region Ω_2

We shall denote the concentrations for glucose, oxygen, and acetate [Glu], $[O_2]$, and [Ac] by $C_g = C_g(\vec{r}, t)$, $C_o = C_o(\vec{r}, t)$, and $C_a = C_a(\vec{r}, t)$, respectively, where $\vec{r}$ denotes the position vector of a spatial point in agar or colony, and t denotes time. The reaction-diffusion equation for each of the concentration field $C_g = C_g(\vec{r}, t)$, $C_o = C_o(\vec{r}, t)$, and $C_a = C_a(\vec{r}, t)$ has the following general form (refer to Fig. 1):

$$\partial_t C = D_- \Delta C \qquad \text{in agar region } \Omega_- \ \dots (1)$$

$$\partial_t C = D_+ \Delta C + \rho P - \rho Q \qquad \text{in colony region } \Omega_+ \ \dots (2)$$

$$C_- = C_+ \quad \text{and} \quad D_- \partial_n C_- = D_+ \partial_n C_+ \ \text{ on the agar-colony interface } \Gamma_{12} \dots (3) .$$

Here, D_- and D_+ are the diffusion coefficients for the substance with concentration C in the agar and colony regions Ω_- and Ω_+, respectively, C_- = C in agar and $C_+ = C$ in colony, respectively, and ∂_n denotes the normal derivative in the direction from agar to colony. If $C = C_g, C_o,$ or $C_a,$ then we denote the diffusion coefficients by $D_{g,-}$, $D_{g,+}$, $D_{o,-}$, $D_{o,+}$, or $D_{a,-}$, $D_{a,+}$, respectively. In the reaction term, $\rho P - \rho Q$, ρ is the local cell density, and P and Q are the production and consumption rates defined in the colony. We model these rates for the concentrations $C = C_g, C_o,$ and C_a , by

$$P_g = 0 \text{ and } Q_g = \left[q_{g,aer}\lambda_{g,aer}\theta_g\theta_o + q_{g,ana}\lambda_{g,ana}(1-\theta_o)\right]\theta_g\left(1-\tilde{\theta}_a\right) \dots (4)$$

$$P_o = 0 \text{ and } Q_o = \left[q_{o,g}\theta_g\lambda_{g,aer}\theta_g + q_{o,a}\left(1-\theta_g\right)\lambda_{a,aer}\theta_a\right]\theta_o\left(1-\tilde{\theta}_a\right) \dots (5)$$

$$P_a = \left[p_{a,aer}\theta_g\lambda_{g,aer}\theta_o\theta_g + p_{a,ana}\lambda_{g,ana}(1-\theta_o)\theta_g\right]\left(1-\tilde{\theta}_a\right) \dots (6)$$

$$Q_a = q_{a,aer}\left(1-\theta_g\right)\lambda_{a,aer}\theta_o\theta_a\left(1-\tilde{\theta}_a\right) \dots (7)$$

respectively. Here, we use the Monod kinetic forms,

$$\theta_g = \frac{C_g}{C_g+K_g}, \quad \theta_o = \frac{C_o}{C_o+K_o}, \quad \theta_a = \frac{C_a}{C_a+K_a}, \quad \tilde{\theta}_a = \frac{C_a}{C_a+K_I} \dots (8)$$

where $K_g, K_o,$ and K_a are the Monod constants for glucose, oxygen, and acetate, respectively, and K_I is the inhibition constant corresponding to the toxic effect of acetate. The parameters $\lambda_{g,aer}$, $\lambda_{a,aer}$, and $\lambda_{g,ana}$ are constant, and they represent the maximum constant cell growth rates for aerobic growth on glucose, aerobic growth on acetate, and anaerobic growth on glucose, respectively. All subscripted p and q are also constant parameters: $q_{g,aer}$ and $q_{g,ana}$ are the specific uptake rates for glucose in the aerobic and anaerobic growth, respectively; $q_{o,g}$ and $q_{o,a}$ are the specific uptake rates for oxygen in the aerobic growth on glucose and that on acetate, respectively; $p_{a,aer}$ and $p_{a,ana}$ are the specific production rates for acetate in aerobic and anaerobic growth, respectively; and $q_{a,aer}$ is the specific uptake rate for acetate in aerobic growth.

The system of equations (1)-(3) are supplemented with the boundary and initial conditions. The boundary conditions for the concentrations of glucose C_g and acetate C_a are the flux-free on all the boundaries surrounding the colony and agar regions, i.e.,

$\partial_n C_g = 0$ and $\partial_n C_a = 0$ on $\Gamma_{01} \cup \Gamma_{02} \cup \Gamma_s \cup \Gamma_b$,…(9)

cf. Fig. 1. The boundary conditions for the concentration of oxygen are

$\partial_n C_o = 0$ on $\Gamma_s \cup \Gamma_b$ and $C_o = C_{o,0}$ on $\Gamma_{01} \cup \Gamma_{02}$,…(10)

Where, $C_{o,0}$ is a constant oxygen concentration. Initially, the glucose concentration C_g is set to be a constant in the agar region, but the initial value of the oxygen and acetate concentrations C_o and C_a are set to be 0.

We denote by $\lambda = \lambda(\vec{r}, t)$ the local cell (mass) growth rate at a spatial point $\vec{r}$ in the colony and time *t*. This is a basic quantity that connects the continuum and discrete parts of our hybrid model. It is given by

$$\lambda = \left[\left(\lambda_{g,aer}\theta_g\theta_g + \lambda_{a,aer}\left(1-\theta_g\right)\theta_a\right)\theta_o + \lambda_{g,ana}\theta_g(1-\theta_o)\right](1-\tilde{\theta}_a)\ldots(11)$$

Here, the term $\lambda_{g,aer}\theta_g\theta_g + \lambda_{a,aer}(1-\theta_g)\theta_a$ describes the rate of aerobic growth on glucose and acetate, and the term $\lambda_{g,ana}\theta_g$ describes the rate of anaerobic growth on glucose. The last term $(1-\tilde{\theta}_a)$ describes the toxic effect of acetate on the cell growth.

Regarding the numerical solving algorithm, our simulation is done through a time iteration with a time step Δt. Each iteration consists of the following main steps:

(1) Given the configuration of all the individual cells (i.e., their spatial coordinates) in the colony, we determine a coarse-grained, smooth colony boundary.
(2) We solve the system of reaction-diffusion equations in both the agar and colony regions to update the concentrations of glucose, oxygen, and acetate.
(3) We update the local growth rate for cells in the colony region; and
(4) Simulate the growth, division, and movement of all the individual cells in the colony with another iteration of a different and smaller time step of size δt.

1.3 Results

Exponentially growing non-motile, non-EPS producing and GFP labelled E. coli K-12 NCM 3722 cells (detailed strain info in Materials and Methods Section 1.2.1) in batch cultures containing 20mM Glucose and 10mM NH_4Cl were used to seed the colony on minimal media agar plates (1.5% w/v agar concentration) that has the same concentration of carbon and nitrogen sources as in the batch cultures (For detailed info relating to the agar plate parameters such as volumes, thickness etc. refer to Materials and Methods Section 1.2.2). The colony density on the agar plates was carefully controlled such that average colony distance between the center of two colonies was not less than 1 cm. The plates were stored in incubator at 37^{o}C and were only taken out for confocal microscopy imaging, with only those colonies being chosen for viewing that fit the criteria above. From the images acquired by the confocal z scans, radius and height of the colony were computed using the colony profiles. We also implement an agent-based model similar to our earlier study in Warren et al, 2019[3], with additional implementation of effects of effects of anaerobic growth and cell maintenance but with reduced dimensions. The simulated colony begins from a single cell akin to the experiments with agar dimensions of 1.6cm length x 4mm agar depth (refer to Materials and Methods Section 1.2.4 for details about the model).

1.3.1 Experimental colony radius, height and profiles measurements

We measured the profiles of the colony growing on agar (1.5% w/v) containing an initial glucose concentration of 20mM at various time points starting from the initial single-cell seeding process for a period up to 3 days, using our confocal microscopy setup. These profiles were computed using the confocal z-scans with the radius at a particular height being determined by fitting a circle to pixel intensities in the image that were above a threshold value. The radius of the colony is defined as the maximum radius across all the z scans, with the height being defined by the distance between the maximum radius and the colony top at which the radius is zero (see Materials and Methods Section 1.2.3 for details).

Warren et al, 2019 [3] described the linear vertical and horizontal expansion speeds of the colonies in the initial 24 hours, with a slowdown occurring in the vertical component after that. Here we allowed the colonies to expand further till 72 hours, and observed that while there was no slowdown in the radial expansion speed in the timespan of our measurement, vertical expansion slowed down considerably beyond a height of around 250 µm. (Fig 2a and Fig 2b). The results from the agent-based colony simulation, which uses metabolic parameters determined from batch culture, reveal a similar trend, as shown in Fig 2c and Fig 2d. Absolute value differences in radius and height of the colony are attributed at least in part to the fact that the model was simulated in (1+1) dimensions. This reduction in dimensions was made to reduce the computational cost of simulating such large colonies.

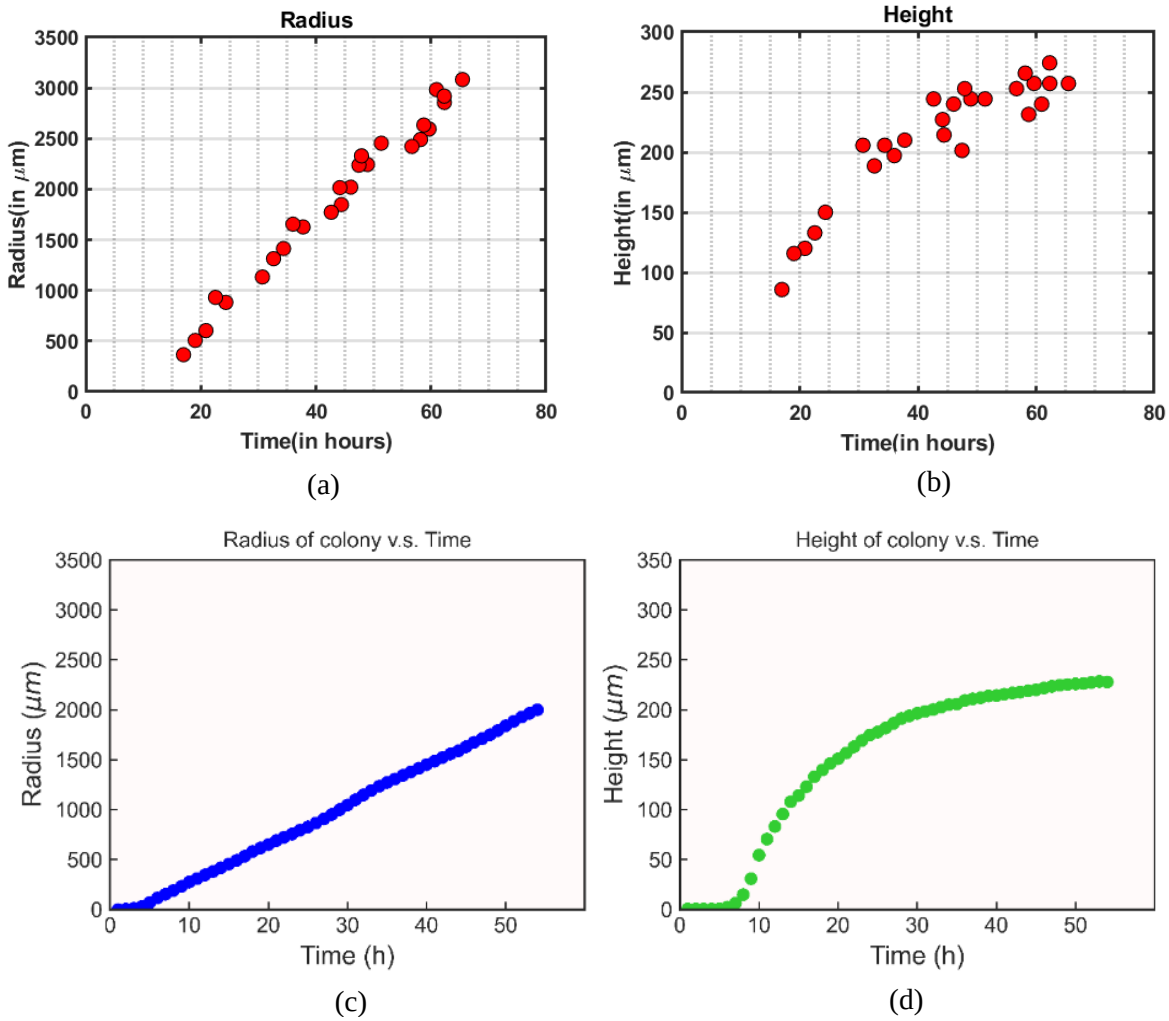

Figure 2: Radius and Height obtained from the (a), (b) Experimental Colony growth and (c), (d) Simulated agent-based model

The experimental colony profiles (Fig 3a) show the colonies having a dome- shaped structure, with the radial dimensions being close to an order of magnitude times more than the vertical dimensions by around 50 hours. The profiles are plotted for alternate sequential timepoints for better clarity, beginning from around 17 hours to about 50 hours. Note that since we use colonies from different plates, some consecutive profiles might differ slightly in their shapes, like the ones at about 36 and 43 hours. The reason for other discrepancies like the difference in the curvature near the colony top, which can be seen for the earlier mentioned profiles, is currently unclear and still under study. The profiles for the agent-based simulation was obtained using a similar approach that was used to obtain the experimental profiles, and are shown in Fig 3b. The model is able to qualitatively and semi-quantitatively capture the dome-shaped profile of the colony.

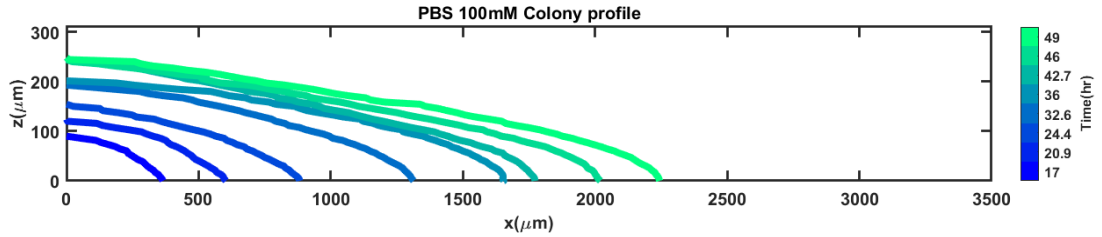

(a)

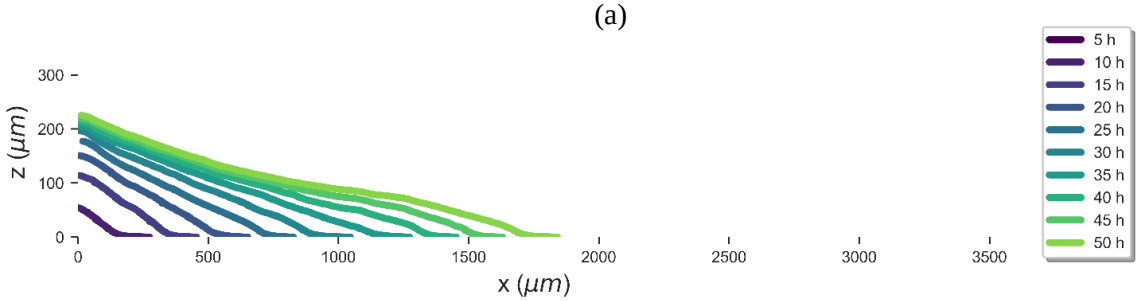

(b)

Figure 3: Experimental and Simulated Spatial Colony Profiles.

1.3.2 Nutrient profiles and Growth zones in the colony

We then looked at the spatial profiles of the metabolites- glucose, acetate and oxygen from the agent-based simulation as the colony growth occurs, and they are shown in Fig 4. We also classified these colony regions on the mode of growth that was taking place based on the local concentrations of these metabolites, depicted in Fig 5.

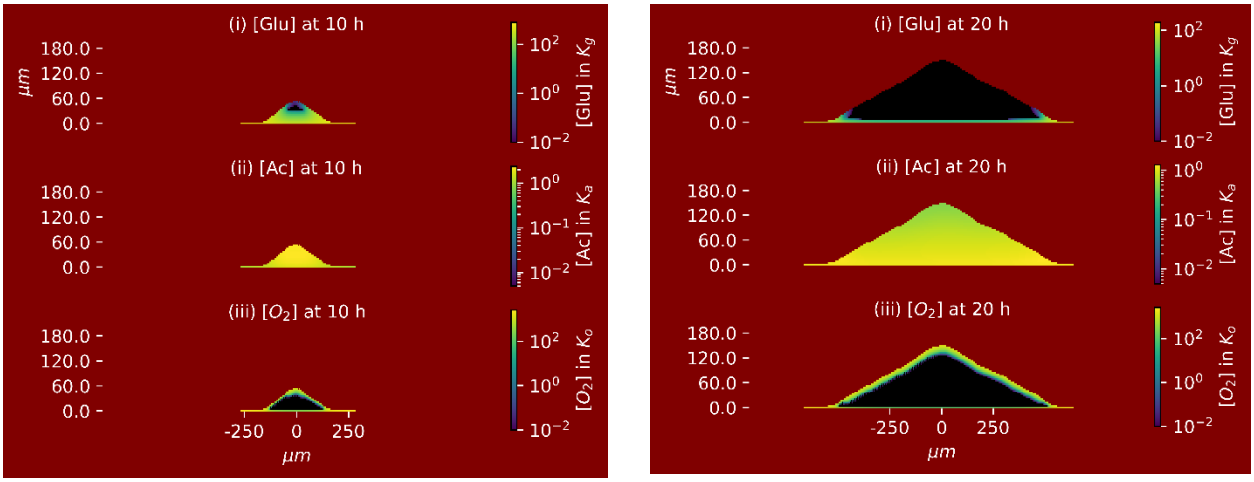

(a) (b)

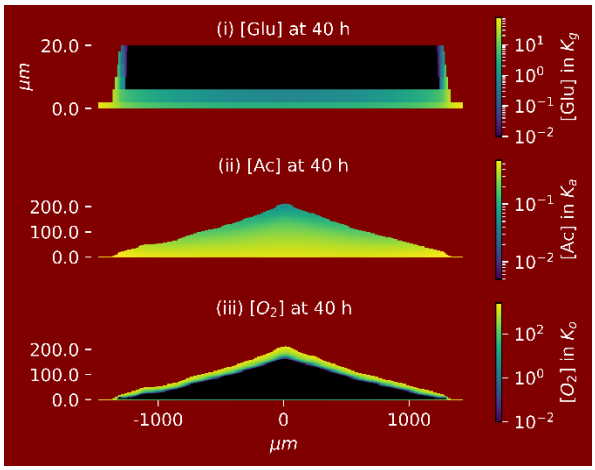

(c)

Figure 4: Colony profiles with color gradients indicating the concentration of glucose (top panel in each subfigure), acetate (middle panel) and oxygen (bottom panel) in units of their respective Monod constants at (a)10h (b)20h and (c)40h. Note that the profiles for the top panel in (c) are zoomed in near the colony bottom as glucose concentration is non zero only in these regions close to the agar

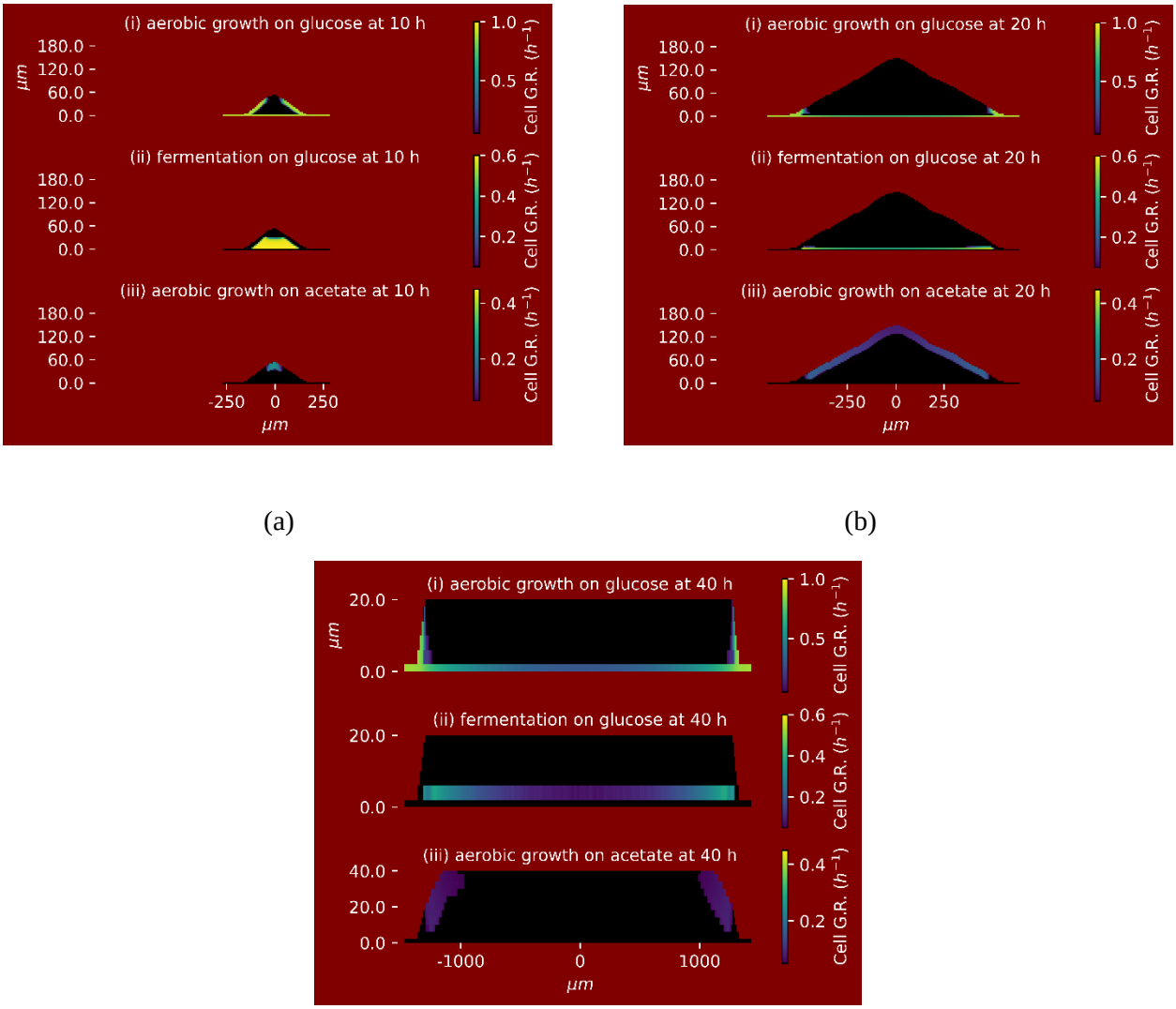

(a) (b)

(c)

Figure 5: Colony profiles with color gradients indicating the growth modes of Aerobic metabolism on glucose (top panel in each subfigure), fermentation on glucose (middle panel) and aerobic growth on acetate (bottom panel) at (a) 10h, (b) 20h and (c) 40h. Note that the profiles in all the panels in (c) are zoomed in near the lower part of the colony as the growth rate is non zero only in these regions.

The concentration of the metabolites is shown in terms of the local levels compared to its Monod constant, as it's a good indicator of the local growth rate of the cell compared to the maximal growth rate. For glucose, the Monod constant is taken to be 20μM [11], the value for acetate is taken to be 5mM (which was measured in batch cultures, data shown in Supplementary Fig S1) and for oxygen we use 0.1 μM. As

discussed in Section 1.2.3, our model has three predominant growth modes- aerobic growth on glucose, anaerobic growth on glucose and aerobic growth on acetate. Firstly, we notice that throughout the process of colony growth, oxygen is restricted to the colony boundaries, resulting in aerobic growth along these regions. (Fig 4a, 4b and 4c bottom panels) In the initial hours of growth, the colony grows predominantly on glucose (Fig 5a top and middle panels), resulting in glucose depletion in the upper layers near the center of the colony (Fig 5a, top panel). This depletion in glucose near the colony top is visible as early as 10 hours mainly due to the fact that the size of this region results in a higher glucose uptake flux compared to other regions. Also, a key factor contributing to this depletion is the restriction of oxygen to just the top and bottom layers, thereby restricting aerobic growth on glucose to just these regions. Most of the colony interior grows anaerobically on glucose, and since anaerobic metabolism on glucose requires a lot of glucose uptake for the production of similar amounts of energy and biomass as aerobic metabolism, the depletion in glucose in the colony interior starts to occur. (Fig 4a and Fig 4b, top panels).

Anaerobic metabolism also results in a buildup of byproducts of fermentation like acetate which diffuse throughout the colony (Fig 4a middle panel). A point to note is that oxygen is abundant near the colony top. (Fig 4a bottom panel). Since the glucose concentration is low near the center of the colony while the acetate concentration is high, the cells in these regions grow aerobically on acetate (Fig 5a, bottom panel).

At 20h, we can see that most of the glucose is depleted from the colony, and restricted just to the expanding edges (Fig 4b top panel), and since oxygen is abundant here on the frontier, the cells continue to grow aerobically on glucose at the periphery of the colony, thereby maintaining the radial expansion rate. (Fig 5b top panel). The other regions abundant in oxygen, the entire colony top, now grow on acetate since glucose is not available in these regions (Fig 5b bottom panel). As the colony continues to grow on acetate, acetate also gets depleted from these top regions, falling to levels far below the Monod constant for acetate uptake, thereby leaving the regions growing on acetate to be just the colony sides near the periphery at 40h

(Fig 5c, Bottom panel). Aerobic growth on glucose continues to occur in a thin layer along the expanding edges of the colony, and anaerobic growth in few layers near the bottom of the colony.

1.3.3 Possible effects of acetate on colony growth

As the simulations indicate that major portions of the colony grow on acetate, we wanted to test the possible effects of acetate metabolism on colony growth experimentally and thus designed two experiments. Firstly, we grew the colony on different concentrations of the phosphate buffer, to test the toxic effects of acetate on the pH of the colony which would be enhanced under low buffer conditions [12]. Secondly, we tested the effects of *aceA* gene deletion from our strain- *aceA* encodes for the enzyme isocitrate lyase, an important enzyme in the glyoxylate shunt, and allows the growth on acetate to take place in *E. coli* avoiding the decarboxylation steps of the TCA cycle.

The colony radius and height for low phosphate buffer concentrations ranging from around 10-30mM are plotted together with the concentrations used normally in our experiments – around 100mM in Fig 4a and Fig 4b. We observe that while the radius of the colony is mostly unchanged across the buffer conditions, the height of the colony shows different behavior for all the 3 buffers that we tested. The 10mM

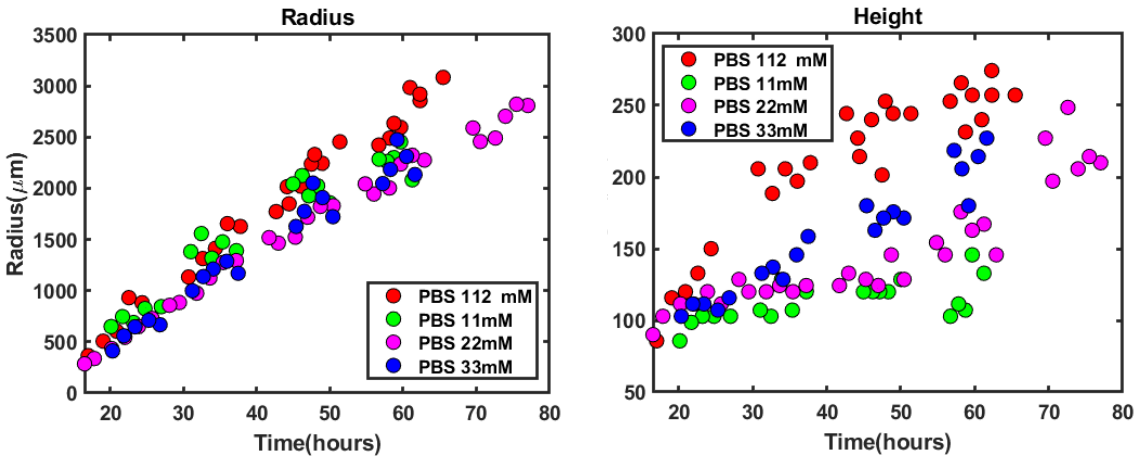

Figure 6: Experimental radius and height comparison for different concentrations of buffer

buffer case saturates at a low height not much beyond 100µm, while the 20mM and the 30mM although being initially lower (before 40 hours) than the 100mM buffer, rise gradually to eventually reach about the same height, with the rise slower for the 20mM buffer compared to the 30mM case.

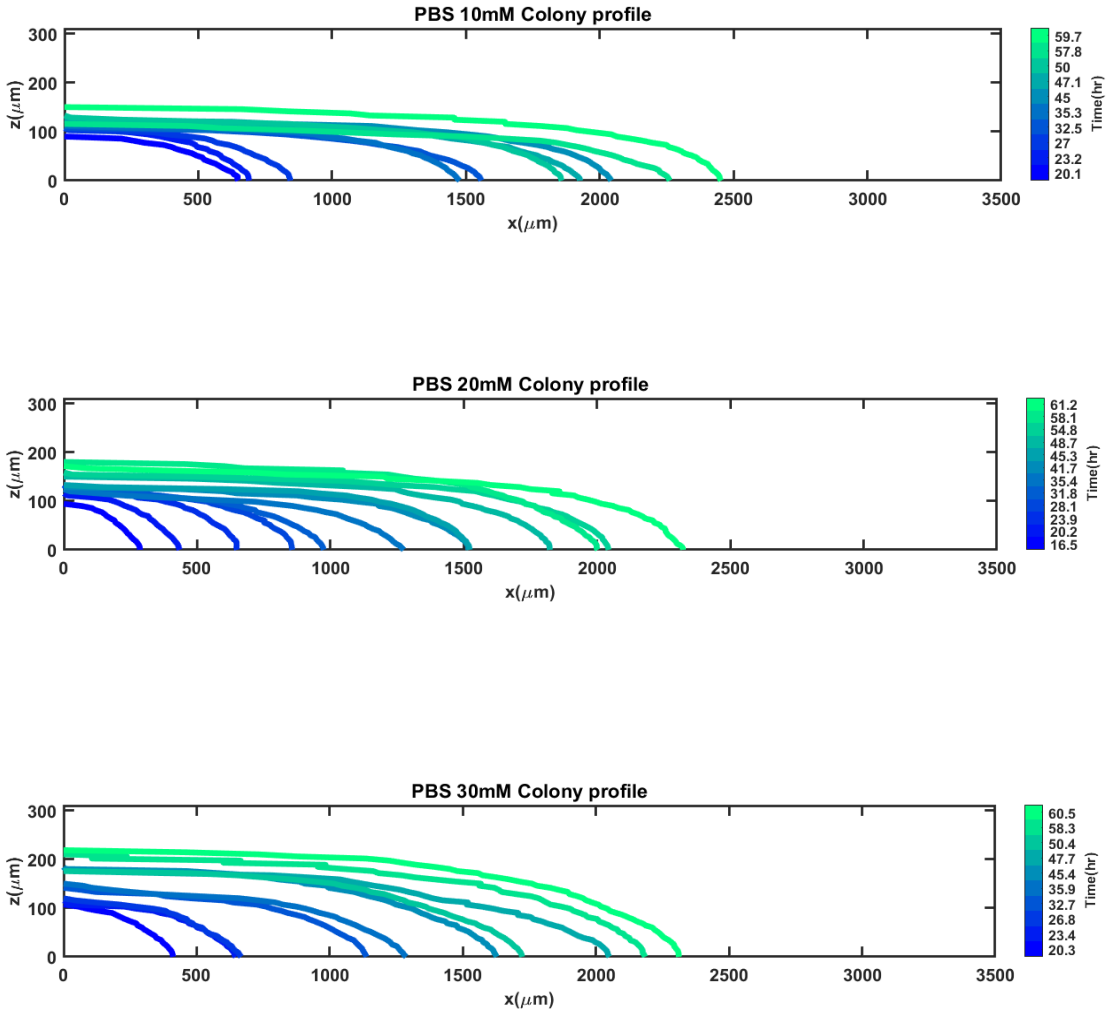

Figure 7: Experimental colony profiles for different concentrations of phosphate buffers

The profiles of the colony also show qualitative differences compared to the ones shown in Fig 3a. Instead of a dome shaped, the 10mM case represents a flat top (Fig 7 top panel), while the 20mM and 30mM resemble a flat top in the initial timepoints (Fig 7 middle and bottom panels) but slowly converge to having similar dome- shaped profiles as in the higher buffer conditions.

The deletion of *aceA* gene surprisingly did not affect the colony radius and height, as is shown in Fig 8. The profiles are also similar to the wild type case (Fig 3a), with the dome shaped colony structure. Across the 70-80 hours when the colonies were imaged in our study, the mutant and wild type strains colony profiles are pretty similar. These results, the dependency on the buffer conditions and the role of acetate uptake, are currently still being investigated by the agent-based model by including toxicity and turning of acetate uptake in the simulations respectively.

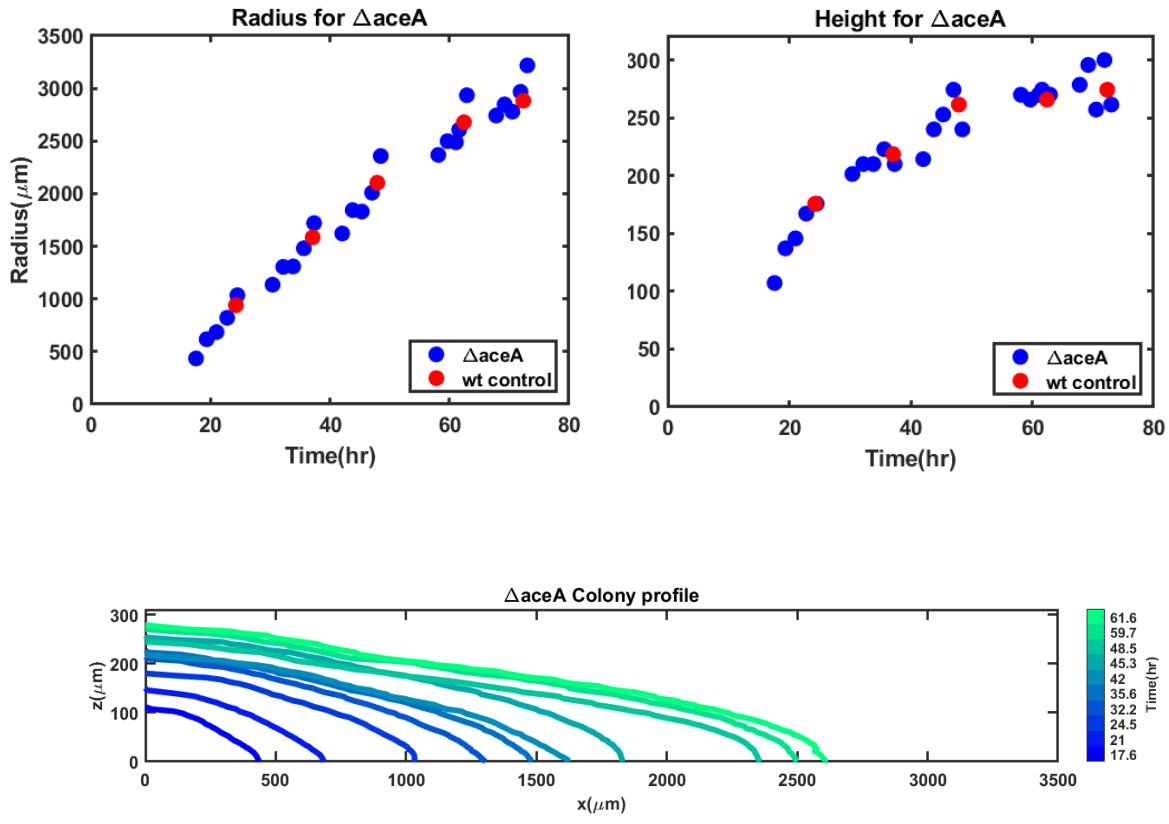

Figure 8: Showing the colony radius and height measurements along with profiles for Δ*aceA* strain

1.4 Discussion

In this Chapter, we focused on studying the growth of a colony beginning from a single *E. coli* cell, specially trying the understand the factors which govern observable quantitative characteristics of growth like radial and vertical expansion speeds. Our model builds upon the prior work by Warren et al, 2019, with an emphasis on the metabolic aspect of colony growth as in the interplay between the metabolite's glucose, acetate and oxygen as the colony growth occurs in time. Our experimental observations reveal that the radius of the colony continuously increases linearly throughout the span of our experiment (around 70 hours), but the vertical expansion slows down after about 24 hours and begins to saturate at 250-300μm. The colony profiles show a dome like shape with a height-to-length ratio of around 1:10. We are able to capture this behavior with our agent-based model, although semi-quantitatively due to approximations made by reducing the model to (1+1) dimensions. The computed spatial metabolic profiles of the colony suggest that glucose consumption is the main source of growth for the colony in the initial 10 hours of colony growth, a major part of which is through fermentation in the interior regions of the colony devoid of oxygen, thereby producing fermentation byproducts like acetate which diffuses inside the colony. As the glucose gets depleted in the colony interior, the cells at the top layers exposed to oxygen start to grow on acetate. This is followed by lowering of acetate levels near the colony top restricting growth through acetate consumption on the top sides of the colony. Also, the cells at the expanding edge of the colony continue to grow aerobically on glucose, and do not face limitation due to nutrient diffusion, with glucose concentrations being far above the K_s for glucose.

We then tried to test some of the model predictions experimentally by examining the role of acetate on colony growth. We lowered the concentrations of phosphate buffer to see the toxic effects of fermentation byproducts, majorly acetate. Acetate can cause a toxic effect in the growth of the colony by lowering the pH of the medium, and thus the effects of its excretion is more pronounced in low-buffer environments. The colonies in the low buffer scenario displayed vastly different spatial profiles with a

flatter top, compared to the dome shaped profiles seen normally when the buffer concentrations are high. We then tested the colony growth for Δ*aceA* colonies, which cannot utilize acetate for biomass production. The radial and vertical profiles for the deletion mutant were identical to the wild type colonies, with some possible differences occurring after 80 hours. In retrospect, the lack of differences between the mutant and wild type colonies may be attributed to the fact that acetate is not the only fermentation product excreted and diffusing across the colony. Other products such as lactate [13], pyruvate and alanine [14] might play a similar role as acetate.

. We did not investigate further into the growth regime of the colony beyond 70 hours because of the possibility of other factors that we did not take into account like cell death. It however remains an interesting possibility to test in the future, and can help us have a better understanding of physiological factors like cell maintenance and the role it plays in maintaining the viability of cells [15]. There have been a lot of interesting technical innovations in experimental studies on *E. coli* biofilms in recent years [14][16], and future research in this area looks promising.

Acknowledgements

Chapter 1, in part, is in part is currently being prepared for submission for publication of the material with Kannan, Harish.; Caglar, Tolga; Ge, Daotong, Dong, Jiajia; Sun, Paul; Zhang, Zhongge; Li, Bo and Hwa, Terence. The thesis author was a primary researcher and author of this material.

2. Chapter 2: Dynamics of Cross-Feeding *E. coli* colonies

2.1 Introduction

In Chapter 1, we presented the various factors that play roles in the development of colonies starting from a single cell, and the associated heterogeneity across the spatial and temporal scales. In this Chapter 2, we aim to apply our understanding and insights gained from the earlier study to study the development of more complex colonies involving two interacting *E.coli* strains.

Colony growth involving microbial communities with mixed genotypes have often been a recent focus of range expansion studies, owning to the various evolutionary factors at play including genetic drift, natural selection and dispersal [17][18]. Many studies have shown the dominant role of random genetic drift in these colony expansions as populations at the front divide more rapidly owning to the relatively better abundance of nutrients, such that the descendants of these sub-populations make a large proportion of the expansion front. This results in a positive feedback loop, wherein populations once stochastically entering the population front, persist at the front via a "gene surfing" effect [18]. The global spatial structures of these range expansions have a homogenous "core", where populations are evenly mixed and as growth occurs, with is a loss of spatial diversity and formation of discrete "sectors" of individual clonal clades as the colony expands. The fluctuations which propel the population to the expanding front can be biased by a range of factors including nutrient supply, expansion speed, structural surface irregularities, and social interactions between participating populations [19-26].

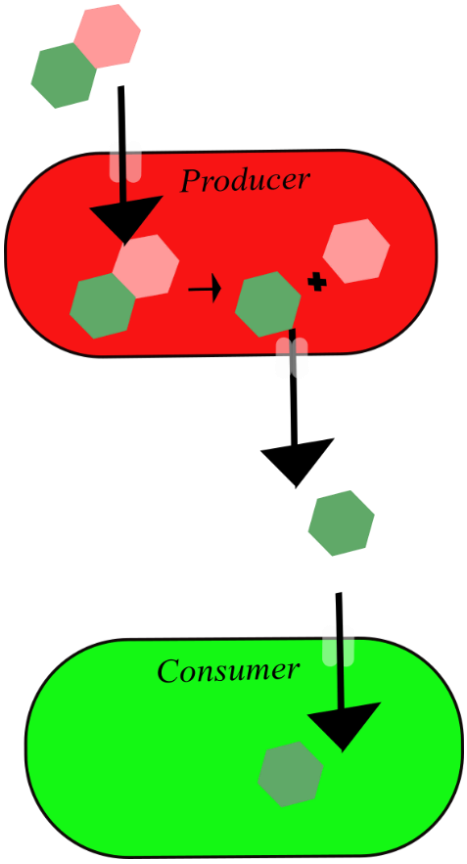

Figure 9: Illustration of cross feeding model system composed of producer and consumer

Social interactions between individual organisms have long been studied by community ecologists and can be classified mainly into five different classes (here symbol denotes type of interaction: + denotes positive effect, - negative and 0 no effect): commensalism (+/0), mutualism (+/+), predator-prey (+/-). competition (-, -) and parasitism (+, -). These types of interaction can be formed in a microbial consortium through a metabolic "cross-feeding" or exchange of metabolites [20][27][28]. Cross-feeding can influence the spatial diversity of microbial structures and is found in different environmental contexts from hydrocarbon degradation in oil-degrading communities to the utilization of products from fermentation by the microbiome in the human gut [28]. In this study, we consider the effects of commensalism interaction, wherein one community can metabolize and breakdown the nutrients from the environment for the other.

In this Chapter, we study the effect of commensalism in the context of bacterial colony growth. Two synthetically engineered strains of *Escherichia. coli* described in Cremer et al, 2016 [29] was used. The producer-consumer cross-feeding system is illustrated in Fig 9. The producer strain EQ403 can take up the lactose from the environment and break it down into glucose and galactose, but can only metabolize glucose for growth. Galactose is released back into the extracellular environment. The consumer strain EQ386 can utilize galactose but it has the uptake genes for lactose metabolism deleted. In a set up where lactose is the only nutrient available in the environment, the consumer solely depends on the producer for its growth.

Analogous cross-feeding microbial systems have been used in a number of recent studies [20][21][22][25][26]. Goldschmidt et al, 2017 [21] used an engineered version of *Pseudomonas stutzeri* strains that differ in their ability to reduce nitrate from the environment under anaerobic conditions. The intermediate metabolite for the strain that breakdowns the nitrate is nitrite and, nitrite is toxic for this producer strain. They showed that in these types of cross-feeding systems, where the intermediate metabolite is toxic for one of the strains, there was a reduction in local diversity loss or an increase in the number of producer sectors when the toxicity was high due to differences in growth rates at the frontier [20]. Toxic effects of cross fed metabolite can have various confounded effects, with difficulties in resolving the basic causal components impacting a particular behavior. Here we investigate a seemingly much simpler system, with the goal being able to characterize the rules and patterns which govern these cross-feeding interactions in colony growth.

2.2 Material and Methods

2.2.1 Strain and Batch culture conditions

In this study, for the producer strains and the consumer strains, we use the strains EQ403 and EQ386 described in Cremer et al, 2016[29]. Both the strains are on *E. coli* NCM 3722 background and have deletion in the lactose and galactose metabolism genes along with plasmids having fluorescent reporters mCherry and GFP respectively. EQ403 has the gene deletion in *galK* and the plasmid pZA31Ptet-mCherry resulting in a constitutive red fluorescence while EQ386 has the gene for *lac I*, *lacZ* and *lacY* deleted with the plasmid pZA31Ptet M2-GFP giving it a green fluorescent color. Construction of Δ*aceA* mutants for EQ403 and EQ386 were done using the similar process described in Section 1.2.1

The PBS buffer conditions used in cross-feeding colony experiments are the same as those described in Chapter 1. For the nutrient carbon source, lactose and galactose were used for the producer and the consumer respectively, unless specified otherwise. The seed culture conditions are the same as the ones described earlier, different seeds were started simultaneously with the consumer and producer. For growth rate measurements, the inoculum was transferred from the overnight minimal media precultures into fresh minimal media at an OD ~ 0.02.

2.2.2 Preparation of minimal media agar plates and plate inoculation for colony growth

The agar plates that were prepared had lactose as the carbon source, at concentrations ranging from 2mM-40mM according to the specific experiment. The lactose concentration by default is kept at 10mM. The agar plates were prepared on the same day as the seed culture with final agar concentration being kept

at 1.5% w/v. For the experiments involving greater agar depth, 16ml of molten agar with minimal media was poured onto petri plates of dimensions 60 mm x 15mm, resulting in the plates having a depth ~8 mm. For the experiment involving lower agar volumes, different amounts of molten agar ranging from 2ml-8ml was poured onto Willco Wells glass-bottom agar plates of dimensions 50mm x 7mm. The default agar volume in these agar plates was 6ml unless specified otherwise, which corresponds to an agar depth of about 4 mm. The drying and storage of agar plates are the same as described in Chapter 1.

For experiments involving inoculation of agar plates, fresh cultures were inoculated from the corresponding precultures (having lactose and galactose as the carbon sources at 10mM concentration for the producer and the consumer respectively unless specified otherwise) such that the initial OD would be around 0.05-0.1. The fresh cultures were allowed to grow exponentially for some time and OD measurements were taken at 2-3 timepoints to ensure that the cultures were growing at their regular growth rates and there were no faster or slower growing mutants. When the cultures were around an OD ~ 0.3, 1ml of cultures of producer and consumer were collected in Eppendorf tubes and were centrifuged at 13.3k rpm and resuspended in PBS buffer. The OD was measured after washing and adjusted so that it was the same for the consumer and the producer and equal volumes ~ 50-100 µL were transferred to a new Eppendorf tube. This was done to ensure that the ratio of the producer and the consumer cells were 1:1 by cell mass. The tube was vortexed for around 5-10s and 0.5 µL of the culture was used to inoculate the center of the prewarmed agar plates. Note that for experiments involving different inoculation densities, appropriate dilutions were made from this Eppendorf tube to a new tube, and the rest of the inoculation process is similar to the one described earlier. The plates were dried in front of the flame on the bench for around 5-10 minutes and dried again in the PCR hood for around 10 minutes. Plates were then wrapped in parafilm and stored in the 37°C incubator until further measurements with confocal microscopy. Most of the experiments were done in replicates with around 2-5 plates having the mixed coculture inoculum from the same tube to ensure that the experiments were reproducible. Confocal microscopy measurements were collected around every 24 hours, with each scan taking between 5 minutes to 40 minutes depending upon

the stage of colony growth, and the plates were wrapped and put back in the incubator as soon as the experiments were completed to avoid agar loss due to evaporation. All the plates were stored at 4^{o}C for a few days after about 8 days from colony inoculation to stop the metabolism of the colony and to allow oxygen to reach the bottom of the colony, which were then imaged again using the confocal microscope. Firstly, as usual, the colonies were imaged through the air-colony interface, and the image is called the "top view". Then we imaged the colonies through the agar-colony interface, with the image being denoted as the "bottom view". The bottom-view of the colonies could only be obtained only for the Willco Well agar plates that were used for experiments involving agar volumes 2ml-8ml. Bottom view images for larger plates that were used for experiments containing 16ml of agar could not be captured in this way possibly due to scattering of light through the thicker agar plates.

2.2.3 Monod Constant Measurements

For measurement of the Monod constant for lactose and galactose for the producer and the consumer respectively, seed cultures were prepared similar to as described earlier. For the measurement of growth rates at relatively high nutrient concentrations(>1mM), precultures were prepared at the same concentrations as the ones in the final experiment. For measurements at concentrations lower than 1mM, the precultures had the carbon source at 10mM, since total cell density from the overnight precultures at concentrations lower than 1mM is lower than the range measured using the UV-Vis Spectrophotometer, and nutrients are depleted earlier when lower concentrations are used so the growth conditions would not exponential. 1ml of the precultures were centrifuged and washed twice with PBS buffer to ensure that no galactose or lactose is transferred over when inoculating the fresh cultures. The inoculum from the washed precultures were transferred at the appropriate dilutions based on rough estimates of Monod constant such that there would be around 10% drop in nutrient concentration for around 2 doublings. The fresh cultures were kept to adapt to the new environment and grow for a period around 2 hours. After 2 hours, appropriate dilutions were made and around 25-100 µL of the culture was transferred ensuring that there would be

around 200-500 colonies per plate. The plates were allowed to dry for around 10 minutes in the PCR hood and then transferred to the 37°C incubator. This was repeated every hour for around a period up to 6 hours. Colony counts were made after around 24 hours of incubation time, and back calculations were made according to the dilutions to determine the colony forming units per ml of the culture(cfu/ml). Growth rates were determined using a linear fit for log(cfu/ml) and time.

2.2.4 Microscopy and Image analysis

Most of the microscopic set up is same as described in Chapter 1. There are some modifications in the Leica microscopy software set up to accommodate dual laser channels for excitation of the fluorophores GFP and mCherry at 488 and 588 nm wavelength respectively. Two HyD SP GaAsP detectors are used and mapped according to the emission spectra of the GFP and mCherry fluorophores 495 to 545 nm and 590 to 700 nm respectively. The gain of the detector and the laser intensity are adjusted to minimize photobleaching of the fluorophore and oversaturation of the image.

As described earlier, tilescan images were taken through the microscope and the images were stitched together using a custom Python Script. Images were resized using imresize function in MATLAB and the resized image was used back in Python to create videos showing the fluorescence intensity across different z stacks and also to create max intensity images, where the intensity at a pixel location is given by the maximum value across different z scans. Image sequences were also loaded in ImageJ/Fiji to analyze the orthogonal views across the xz and yz slices for z stacks corresponding to image from a particular timepoint. These stacks were also used to create a 3d representation of the colony using the 3d viewer plugin.

2.3 Results

2.3.1 Patterns formed by two strain colonies without cross-feeding interaction

As described in the introduction section of this chapter, past quantitative studies [17] have shown how mixing two genotypes of microbial populations in equal proportions results in the formation of well-defined sectors radiating from a homogenous core, alternating between the two genotypes. Their studies involved using immotile *E. coli* DH5α cells marked by different fluorescent reporters, CFP and YFP. As a control experiment, we tried to emulate this scenario by growing the mixture of our two strains on agar having glucose as the carbon source. Both the producer and the consumer cells can grow on glucose as the carbon source, mimicking a simple, non-interacting two strain system, albeit with slight differences in growth rates between the producer and the consumer (data shown in Supplementary figure S2).

Producer and consumer cells that were exponentially growing by themselves separately in minimal media batch culture tubes containing 10mM glucose were mixed in a 1:1 ratio and inoculated onto minimal media agar plates (agar concentration at 1.5%w/v). The agar plates had glucose concentration fixed at 10mM, and had an agar volume of 16ml. The plates were then stored at 37^{o}C incubator and taken out for imaging around 48 and 72 hours after initial inoculation for imaging using confocal microscopy (see Materials and Methods Section 2.2.2). The max intensity was computed from across all the confocal z scans such that the maximum intensity at a particular pixel location in the image is given by the maximum value for that pixel across all the z values. The z scans were also used to compute the cross section of the colony to get information about the colony cross section profiles (for details refer to Materials and Methods Section 2.2.4).

We can observe the initial homogenous core and the formation of sectors as shown in Fig 10ab and inset of the pattern (Fig 10c) at about 72 hours, and the changes occurring in time only across the expansion

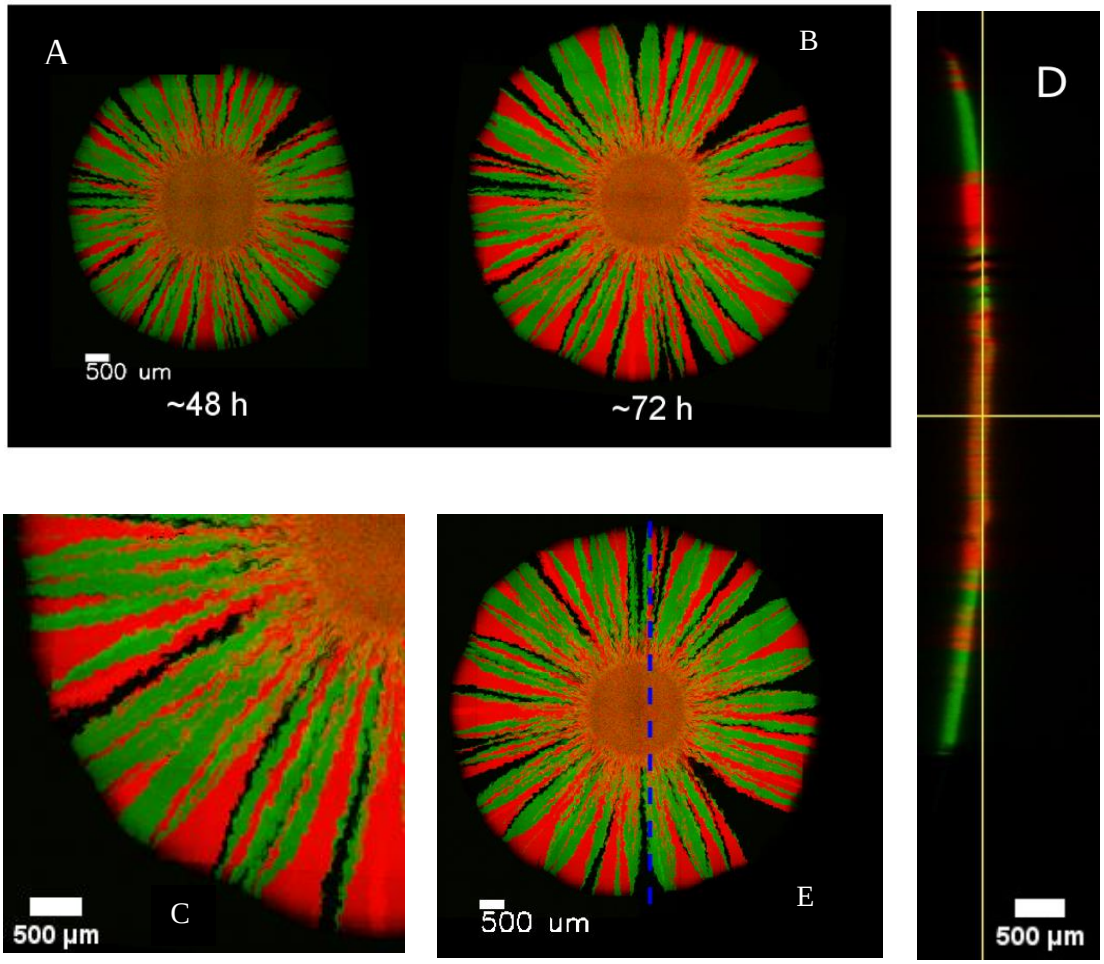

Figure 10: Max Intensity Projections of the colony on the xy plane and yz cross-section for agar plate containing 10mM Glucose with the red color denoting the producer, the green consumer and black regions in the colony depicting plasmid loss. (A) and (B) show the maximum intensity images at about 48 and 72 hours respectively. (C) shows the magnified view of the lower left quadrant in (B). (D) is the yz cross section of the colony at 72 hours along the dotted blue line shown in (E)

frontier. In panel D, we describe the information about the height of the colony obtained from confocal z scans. At a particular z value, the image of the colony can be represented in the xy plane. As we scan across the z plane, we can get information about the height of the colony. Panel B represents a slice of the colony across the yz plane at a particular fixed x value, and along the blue dotted line in Figure 10E. We can see that the profile of the colony looks quite similar to the ones that we had observed in Chapter

1, although the colony sizes are relatively larger compared to those shown earlier. In the single strain colony dynamics study, a colony starts from a single cell, but in our cross-feeding work, we start with ~ 10^5 cells of the producer and the consumer, mixed in a 1:1 ratio. Starting with low cell numbers results in a lot of stochastic heterogeneity in the resulting patterns that develop in the initial inoculation region (data shown in Supplementary figure S3).

Also, across our experiments in this Chapter, we did not add the antibiotic chloramphenicol to the agar plates. The main mechanism for chloramphenicol resistance in bacteria, as is in the plasmid used in our study containing the fluorescent proteins, is through inactivation of the antibiotic through acetylation by Chloramphenicol acetyltransferases (CATs) .As has been shown in the first chapter, acetate excretion during anaerobic metabolism plays an important role in the spatial dynamics of the colony, and we did not want to confound the interactions which could be caused due to the transfer flux for acetylation. Also, only a few sectors showed the loss in plasmid, which did not affect the judgement of qualitative results shown here and the rest of this Chapter. Most of the plasmid loss was in the producer strain. Cross- feeding experiments in which the antibiotic was added at 10µg/ml are shown in Supplementary figure S4.

2.3.2 Patterns formed by colonies of cross-feeding bacteria

Because of the differences in the source of the carbon sources in our cross-feeding system, lactose for the producer and galactose for the consumer, there exists inherent differences in growth rates between the two [29]. The maximal growth rates under saturating amounts of the carbon source are 0.67 h^{-1} for the producer and 0.37 h^{-1} for the consumer respectively. Given this difference, it is not intuitively clear about the possible patterns that could form in space. Kayser et al, 2018[19] showed how despite fitness differences of two populations in terms of growth rates, the proportion of slower-growing strains were more at the population front, propelled by mechanical pushing by neighboring cells. But in our system the consumer is

hence at a twofold disadvantage compared to the producer- a lower growth rate and a reliance on nutrient from the producer to maintain its own growth.

Our experiments involve mixing the producer and consumer cells that were exponentially growing by themselves separately in minimal media batch culture tubes containing 10mM lactose and 10mM galactose respectively, in a 1:1 ratio and inoculated onto minimal media agar plates (agar concentration at 1.5%w/v). The agar plates had lactose concentration fixed at 10mM, and had an agar volume of 16ml, resulting in an agar depth of around 8 mm. The plates were then stored at 37^{o}C and taken out for imaging every 24 hours till a period of 4 days of colony growth after the initial seeding. For the confocal z scan images, max intensity projection and colony cross-section was computed using the method mentioned earlier in Section 2.3.1(for more details refer to Materials and Methods Section 2.2.4)

Our experiments as shown in Fig 11 reveal that at initial timepoints, the producer and consumer both grow in the initial homogenous core, and since only the producer can utilize the nutrients from the agar, it dominates the consumer as shown in the inset in Fig 11c. But despite of the differences in growth rates and reliance upon the producer, consumer cells still are able to arrive at the expanding frontier. As the colony expands with time, the producer starts to mostly occupy the expanding frontier and overtake the consumer. However, we notice that the consumer starts to grow in the interior regions of the colony as is evident comparing the images at 24 and 48 hours. Also, while many “branches” of the consumer are enveloped by the producer as the colony begins to grow, the branches which are thicker at the earlier timepoints take more time to be completely surrounded on the front by producer cells. This ensures that a small proportion of cells at the expanding front are the consumer cells. (Fig 11D)

Looking at the colony from a three-dimensional perspective yields a unique description of the colony, as shown in the colony cross-section view in Fig 11B. The vertical axis depicts the slice of the colony along a particular distance x along the y axis, and the horizontal axis represents the colony height in z-direction. Although the producer and consumer cells were mixed in equal proportions at the start of the experiment, the consumer cells dominate the top of the colony in the interior regions, as is visible by the

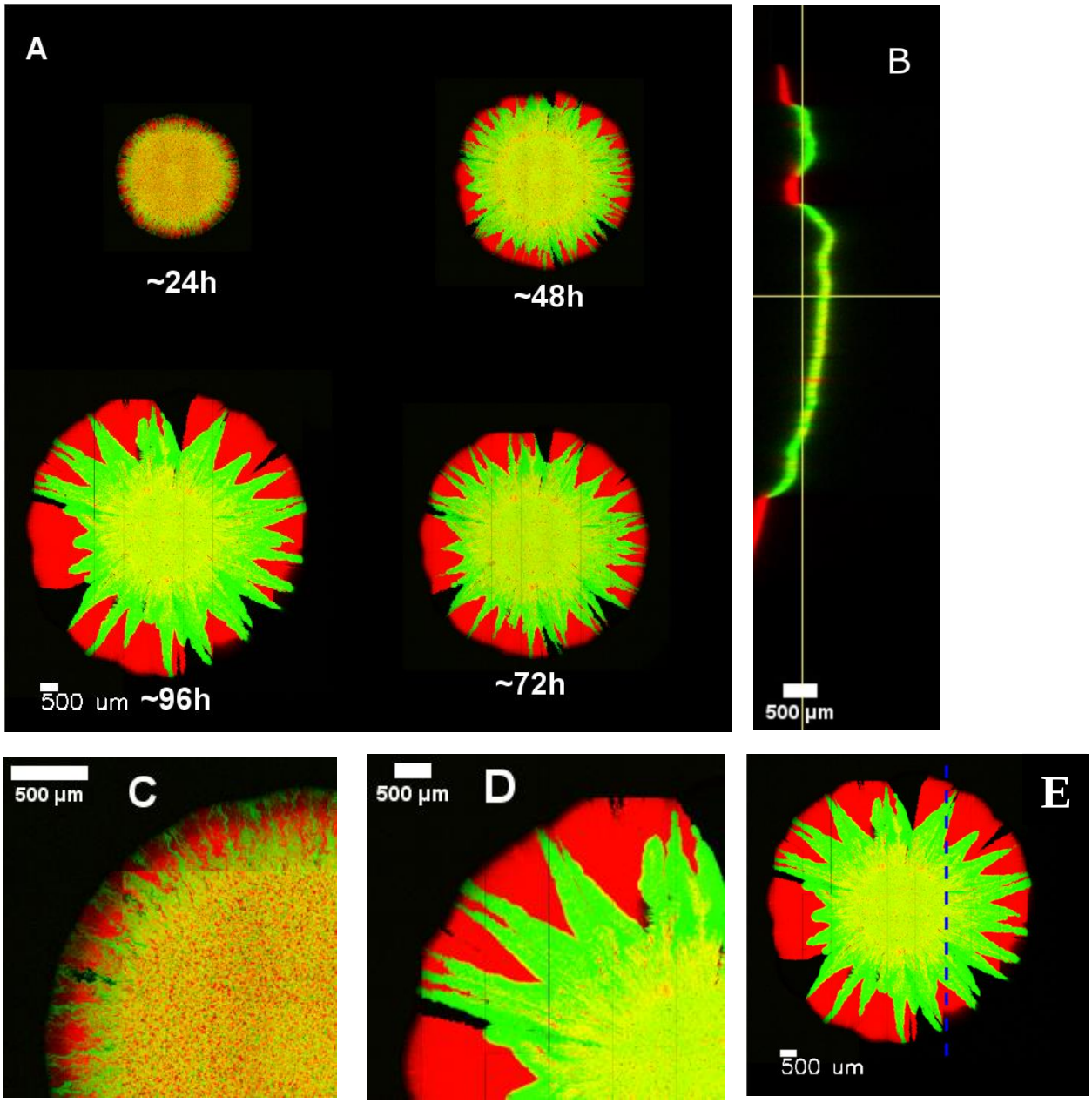

Figure 11: Max Intensity Projections of the colony on the xy plane and yz cross-section for agar plate containing 10mM Lactose with the red color denoting the producer, the green consumer and black regions in the colony depicting plasmid loss. (A) Max Intensity Projections show the growth of the colony starting from 24 hours to about 96 hours after inoculation (B) is the yz cross-section of the colony at 96 hours along the blue dotted line shown in (E) (C) and (D) Shows the magnified view of the upper right quadrant in max intensity projections of the colony shown in (A) for 24 and 96 hours respectively

yellowish-green color in the middle portion of the colony cross-section. As we go from the center towards the colony frontier, i.e., going up or down from the center of the yz cross-section plot, the intensity changes from yellowish-green to green, denoting the colonization of the interior regions by the consumer. As we move further up or down the cross-section, we see the appearance of red intensities, which denotes the population of the producer, with a striking height difference between the green vs the red intensities. This indicates that there is spatial heterogeneity in the distribution of the consumer and producer populations, quite different from the case we saw in Section 2.3.1(Fig 11D) of non-interacting communities.

2.3.3. Appearance of flower-like patterns in nutrient runout conditions

As we saw in the previous section about the consumer overtaking the producer in the interior regions, we then wanted to see what would happen in the scenario if the consumer was given a chance to catch up to the producer. To implement this scenario experimentally, we kept the lactose concentration fixed in the agar but decreased the agar volume in the plates. 6ml of agar was used for these experiments which corresponded to an agar depth of about 4 mm. The experimental results after 4 days of growth are shown in Fig 12. We can see that in the initial 24 hours, there is hardly any difference between this and the scenario shown in Fig 11. But as the colony grows, there are evidently a greater number of consumer "branches" reaching the expanding frontier, which we can deduce by comparing the images around 48 and 72 hours with the images corresponding to the exact same timepoints shown in Fig 11. At 96 hours, an interesting thing happens where these consumer branches which had made its way to the frontier start to occupy the regions previously dominated by the producer. Fig 12c depicts this behavior, and we can observe that the consumer cells grow much further from the center as compared to the producer. The radius of the overall colony as it progresses in time is shown in Supplementary figure S5, and it displays the slowdown of the colony from 48 to 72 hours as compared to the scenario shown in Section 2.3.2, with a relative increase from 72 hours to 96 hours because of the arrival of the consumer at the frontier. This illustrates

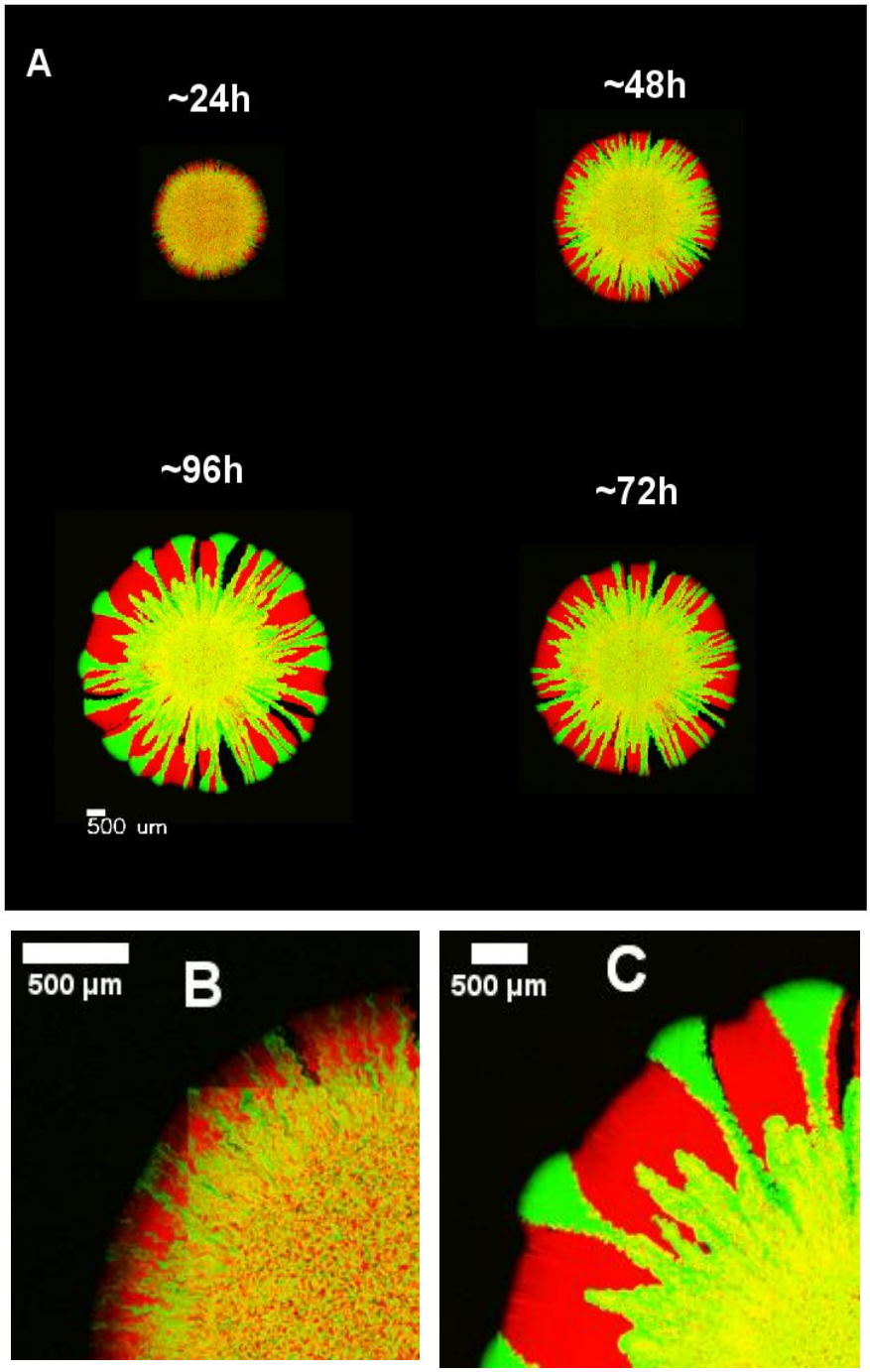

Figure 12: Max Intensity Projections of the colony on the xy plane for agar plate containing 10mM Lactose but with reduced depth of 4 mm with the red color denoting the producer, the green consumer and black regions in the colony depicting plasmid loss. (A) Shows the growth of the colony starting from 24 hours to about 96 hours after inoculation (B) and (C) Shows the magnified view of the upper right quadrant in max intensity projections of the colony shown in (A) for 24 and 96 hours respectively.

that as the colony expands, the nutrient starts to deplete resulting in the slowdown of the producer, and eventually the consumer starts to overlap it.

We let the colonies to grow further after that, to about 8 days to see how things would fare out with the change in dynamics at the frontier. The pattern after 8 days of growth are shown in Fig 13 with the emergence of flower-like patterns. All of the images shown in earlier figures represent the image acquired from the confocal microscope as viewed from the colony-air interface. We also wanted to see the colony distribution in the bottom interior region in the bottom of the colony-which can be obtained by viewing the colony through the agar using the microscope. However, as we have discussed in Chapter 1, the growth mode of the interior region of the colony is mostly anaerobic after the initial 24 hours. Fluorescent proteins GFP and mCherry need the presence of oxygen to fold properly and fluoresce, so we put stored the plates at 4°C to stop the metabolism of the colony which allows oxygen to penetrate in the colony interior. After a few days, the colonies were images through the agar region, and are shown in Fig 13, Panel B. The images acquired from the colony-air interface is shown in Fig 13, Panel A.

We observe that the consumer cells start to expand at the frontier and completely envelop the producer cells. This results in a flower-like pattern with the consumer cells occupying the outermost and innermost layers and the producer cells occupying the middle layer of the colony. There is also spatial heterogeneity as described earlier with consumers at a higher height compared to the producer which can be seen in the yz cross-section slice shown in Fig 13, Panel C and Fig 13, Panel D. Images of the bottom of the colony reveal differences compared to the colony top- the interior regions of the colony seem to be dominated by the consumer when viewed from the top, but indicate dominance by the producer when viewed from the bottom. The exterior regions of the colony dominated by the consumer after nutrient runout, are visible in Fig 13b as well. A detailed version of the 3D rendering of the colony from Figure 13d is shown in Supplementary Video 1.

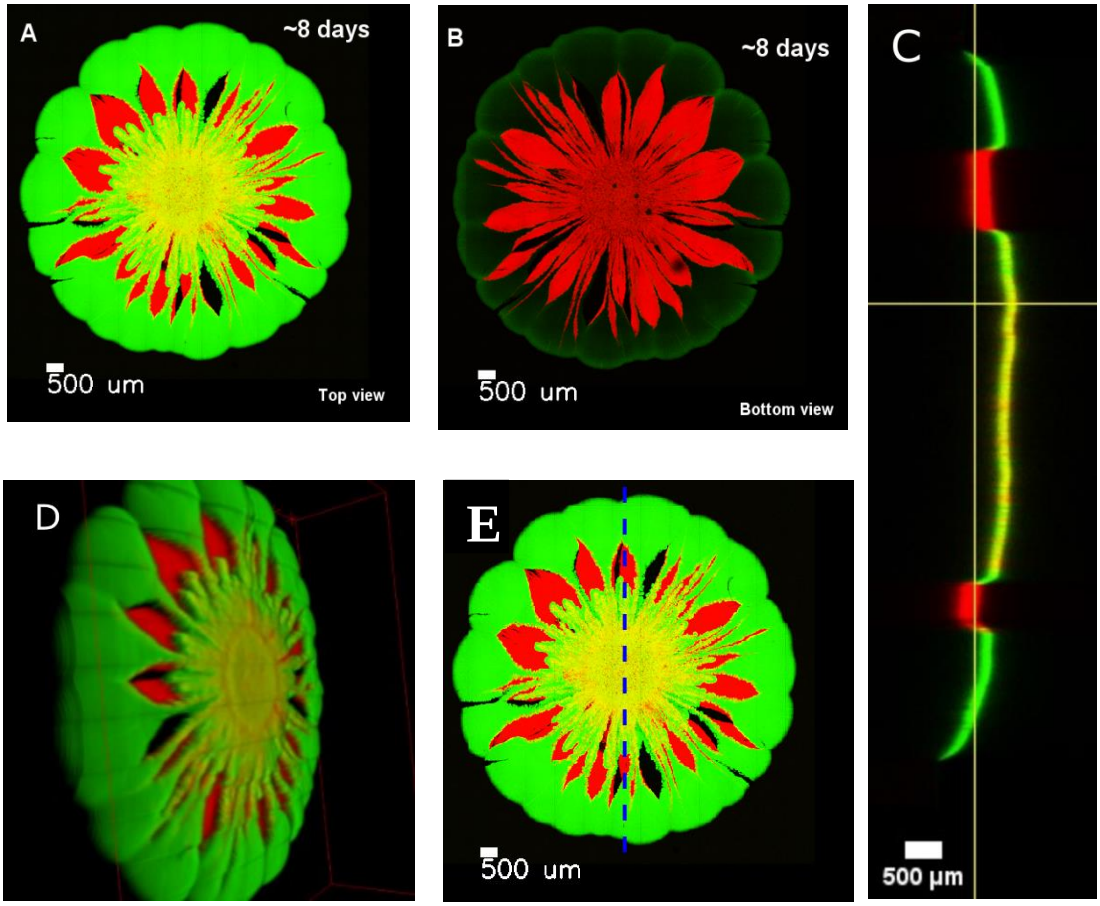

Figure 13: Max intensity projections of the colony on the xy plane showing the formation of flower like patterns after 8 days of growth for an agar Plate containing 10mM Lactose with reduced depth of 4 mm with the red color denoting the producer, the green consumer and black regions in the colony depicting the plasmid loss. (A) Shows the colony image that was acquired by viewing the colony through the air-colony interface in the confocal microscope. (B) Shows the image acquired by viewing through the agar-colony interface. (C) is the yz cross-section of the colony after 8 days of growth across the blue dotted line shown in (E) (D) Side view of the 3-dimensional colony reconstruction made using the 3D viewer plugin in ImageJ. The information about the height of the colony at any particular point is obtained from the confocal z scans.

2.3.4 Dependence on nutrient concentration

Seeing the dependence of nutrient levels on the formation of patterns, we then tried to change the initial nutrient concentrations. We increased the concentration of lactose in the plate from 10mM to 40mM, keeping the agar volume fixed at 6ml. The patterns formed in this scenario are displayed in Fig 14a.

Looking at the pictures at 24 h, we see that a notable change occurs compared to the 10mM case, the color intensity in the initial homogenous "core" changes from yellow in the 10mM case to red in the

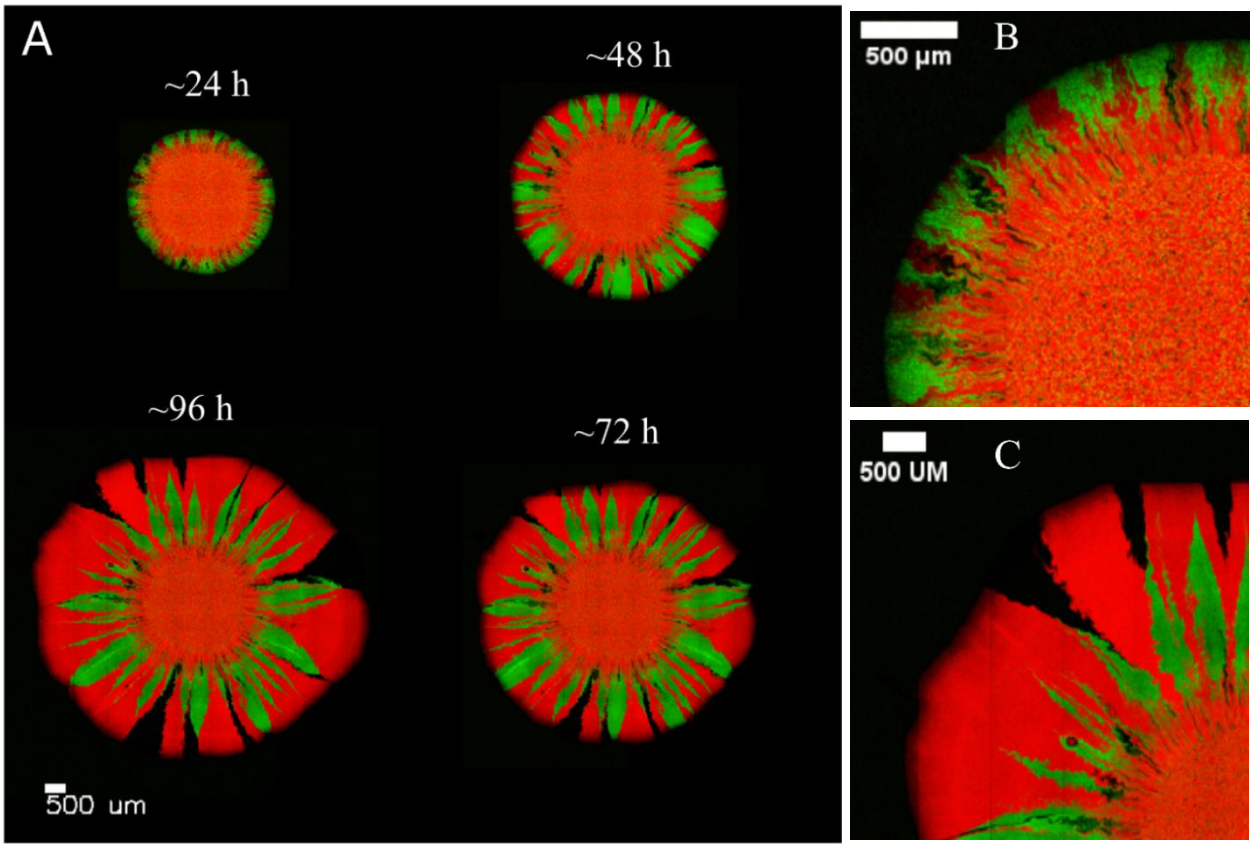

Figure 14: Max Intensity Projections of the colony on the xy plane for agar Plate containing 40mM Lactose with agar depth of about 4 mm corresponding to agar volumes of 6ml, with the red color denoting the producer, the green consumer and black regions in the colony depicting plasmid loss. (A) Max Intensity Projections show the growth of the colony starting from 24 hours to about 96 hours after inoculation (B) and (C) Shows the magnified view of the upper right quadrant in max intensity projections of the colony shown in (A) for 24 and 96 hours respectively

40mM case. Also, there is an apparent reversal in the color intensities at the expanding frontier from red to green. There doesn't seem to be any growth on the top of the colony near the homogenous core for the producer unlike the previous scenario with the consumer. As the colony continues to expand, the consumer branches are eventually overtaken by the producer branches. This is because as was described in Chapter 1, the colonies at the expanding frontier hardly experience any nutrient limitation, and hence the producer is able to overtake the consumer. At later timepoints like 96 h, the producer completely encircles the consumer, exactly opposite to the scenario shown in the earlier section. Thus, entirely different pictures emerge depending on the initial lactose concentration. More experimental results showing the patterns on different agar depths and different initial nutrient conditions are shown in the Supplementary figure S6.

2.3.5 Importance of Monod constant

We looked for a possible explanation for the change in dynamics among the consumer and the producer at the homogenous core region of the colony after about 24 hours of growth (Fig 12B and Fig 14B). Based upon our single strain colony simulations, we know that the as the colony expands, a major portion of the interior colony region grows anaerobically by consuming glucose. This leads to quick depletion of glucose in the interior colony region to values lower than the Monod constant. Thus, in our cross-feeding model, the concentration of lactose in the interior regions might be close to the Monod constant. Monod dynamics for two species with different K_m values and maximal growth rates, with the species having the higher growth rate also having the higher K_m value leads to an interesting scenario shown in Fig 15. On the left-hand side of the intersecting point between the two curves, the species having the lower K_m value has a higher growth rate and on the right-hand side of the intersecting point, the one with a higher maximal growth rate has the higher growth rate, dividing the space into two different regimes.

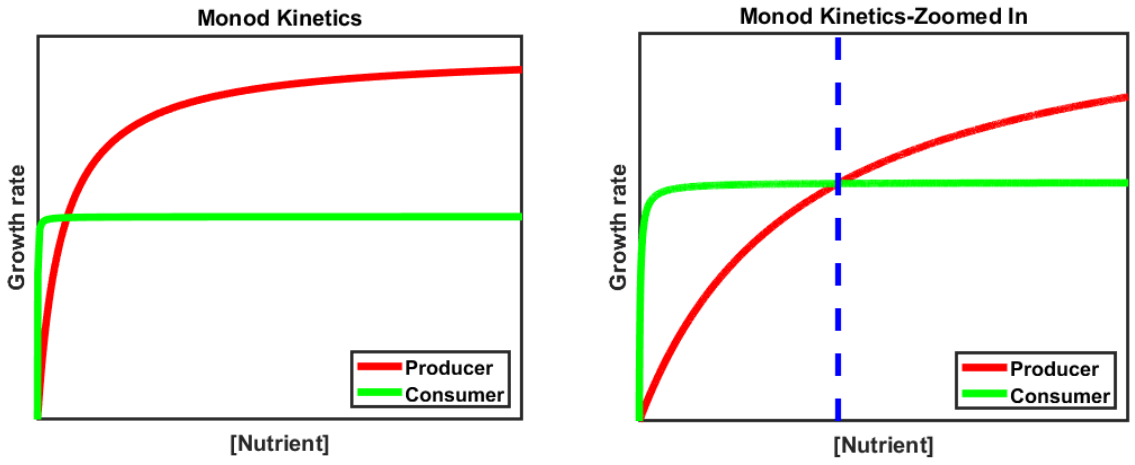

Figure 15: Monod curves for producer and consumer with producer having greater growth rate and higher Monod constant

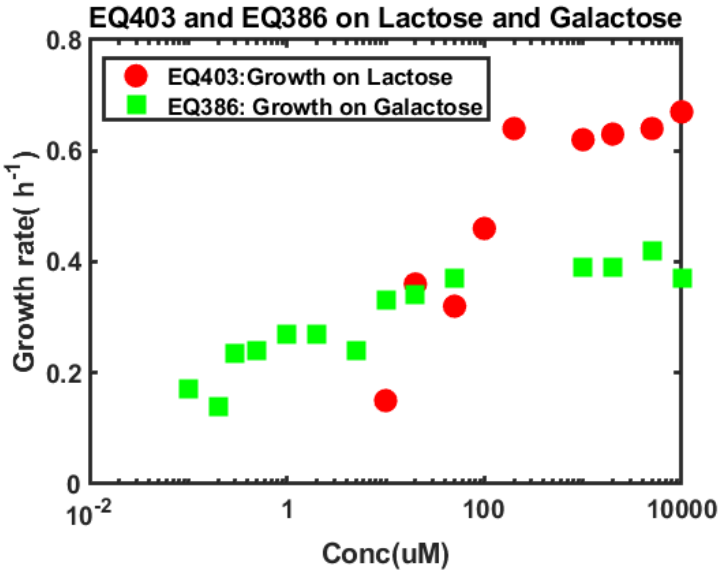

Figure 16: Experimental measurements showing the order of magnitude difference of Monod constants for producer and consumer

We hypothesized that this could be happening in the colonies at 10mM and 40mM concentration. So, we experimentally measured the Monod constants for lactose and galactose uptake for the producer and the consumer respectively and the graphs are shown in Fig 16. These experimental graphs are quite similar to the K_m curve shown earlier, with the multiple orders of magnitude difference between the Monod constants for the producer and the consumer respectively, thus supporting our hypothesis. Our observations

are in agreement with past measurements of Monod constants of lactose and galactose for *E. coli* in chemostats [30] [31].

2.3.6 Role of acetate in helping the consumer reach the expanding frontier

In Section 2.3.4, we reported how the consumer was able to overtake the producer when the nutrient depletion starts to occur in the agar, but a point to note is that even at earlier timepoints like 48 hours (Fig 12a top right panel), some of the branches of the consumer are able to reach the expanding frontier. This is also seen in the scenario where lactose does not get depleted from the agar, i.e., in thicker agar plates shown in Fig 11a. This observation is surprising in the sense that the consumer is able to keep up with the producer despite having a slower growth rate than the producer even at high galactose concentrations. We hypothesized that there might be additional cross-feeding of metabolites, like acetate, in the colony. In Chapter 1, we described the role of acetate in colony growth. Just to summarize, the interior regions of the colony grow anaerobically on glucose in the initial hours of colony growth, building up acetate in the colony, which is then taken up by the colony top at later timepoints. As we have seen the feature of spatial heterogeneity along with the height of the colony in our cross-feeding dynamics, we reasoned that acetate might be playing a role in helping the growth of the consumer on top of the colony.

To test this hypothesis, we first grew both the producer and consumer strains in batch culture, in acetate alone and in lactose or galactose supplemented with acetate. The batch culture experiments of the growth rate of the two strains on acetate reveal similar values for both the producer and the consumer, as shown in Fig 17. But the growth on lactose or galactose supplemented with acetate reveal quite a difference between the producer and the consumer. Lactose seems to be hierarchically utilized first compared to acetate, which is expected since the metabolism of the producer is basically on glucose and glucose is known to be consumed hierarchically with acetate [32][33]. However, the growth rate of the consumer on

acetate and galactose together is greater than the growth rates of either of the two substrates, in fact making it quite similar to the values of the producer on lactose, indicating a simultaneous utilization mechanism. Thus, it provides a basis by which the consumer can catch up with the producer- by growing at similar rates to the producer when both acetate and galactose are available.

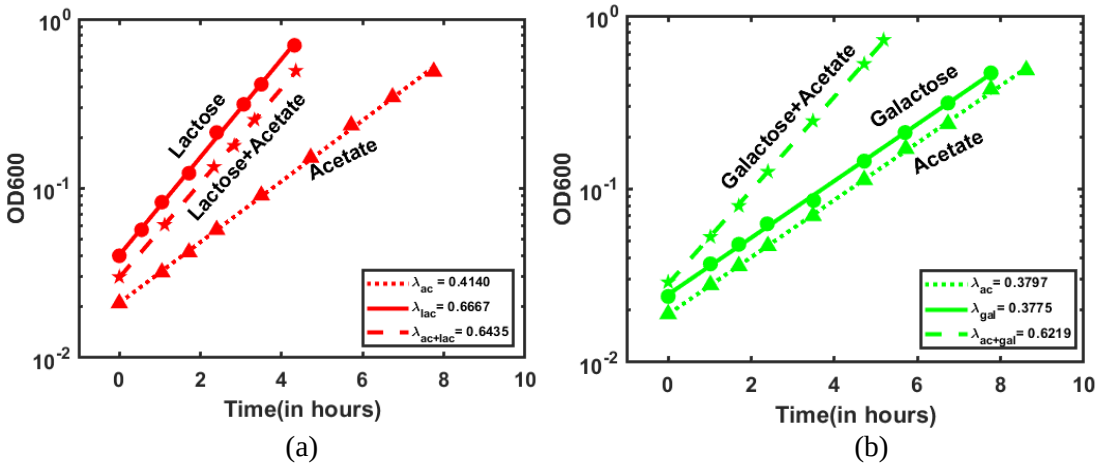

Figure 17: Growth curves of (a)producer strain EQ403 and (b)consumer strain, EQ386 in either lactose/galactose or acetate and on the combined presence of lactose/galactose with acetate

Finally, the role of acetate in the colony can be tested directly by repeating the cross-feeding experiment in the producer and consumer mutants that cannot assimilate acetate for growth. This was done by deleting the *aceA* gene from both the consumer and the producer to stop the growth on acetate. As described in Chapter 1, *aceA* encodes for the enzyme isocitrate lyase, an important enzyme in the glyoxylate shunt, and allows the growth on acetate to take place in *E. coli* avoiding the decarboxylation steps of the TCA cycle. The images shown in Fig 18 depict the max intensity projections for the colony, acquired using the confocal microscope, that initially began with an equal ratio of the mutant version of the consumer and the producer cells that both have *aceA* gene deletions. The agar plate has 10mM lactose with 16ml of agar

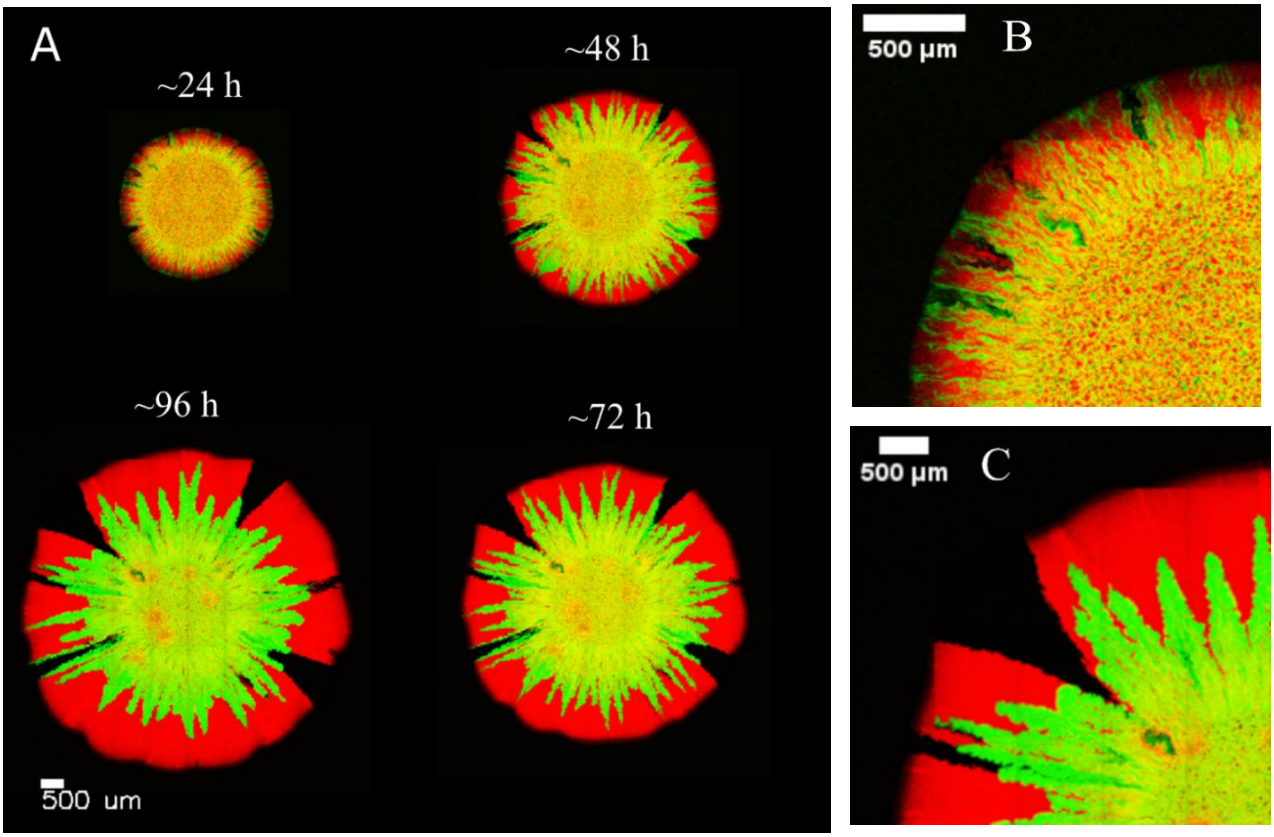

Figure 18: Max Intensity Projections of Δ*aceA* mutant colonies on the xy plane for agar Plate containing 10mM Lactose with agar depth of about 8 mm corresponding to agar volumes of 16ml, with the red color denoting the producer, the green consumer and black regions in the colony representing plasmid loss. (A) Max Intensity Projections show the growth of the colony starting from 24 hours to about 96 hours after inoculation (B) and (C) Shows the magnified view of the upper right quadrant in max intensity projections of the colony shown in (A) for 24 and 96 hours respectively

resulting in a depth of around 8 mm. The experiments were also repeated with lower agar volumes of 8ml (data shown in Supplementary figure S7) and the results were qualitatively similar.

The image at 24 hours seems pretty similar to the images for the experiment without the deletions. However, an interesting scenario emerges around 72 hours- the branches of the consumer fail to reach the expanding frontier of the colony. This results in a complete enveloping of the consumer cells by the producer cells. At 96 hours, we do not observe any of the consumer cells at the expanding frontier, unlike the wild type scenario shown in Fig 11, since there are no consumer cells at the frontier at the initial timepoints to begin with. This experiment reveals the possible importance of acetate metabolism in ensuring

that the consumer cells are around the frontier to take advantage of the lactose runout, envelop the producer, and form the flower patterns.

2.4 Discussion

In this Chapter, we discuss the effects of cross-feeding bacteria growing in a spatially structured environment like biofilms. Our system of study is a simplified version of biofilms- colony growth on agar of *E. coli* cells that do not produce EPS. Our system consists of a producer, which takes lactose from the environment and breaks it down into glucose and galactose, and the consumer, which cannot utilize lactose, feeds on the released galactose that cannot be metabolized by the producer. We observe that even though the producer grows faster on lactose than the consumer on galactose, colonies starting from an equal ratio of the producer and the consumer result in a scenario where the consumer eventually envelopes the producer forming flower-like patterns. Based on our experimental observations shown in the earlier sections, we propose the following scenario which helps in the formation of these patterns:

1) Firstly, the consumer is able to compete with the producer in the initial homogenous core on the first day of colony growth because of the order of magnitude difference in the K_m values of the producer and the consumer for lactose and galactose respectively, with the consumer having a lower K_m. As the colony grows further, the producer continues to grow at the expanding frontier, while releasing galactose which diffuses through the colony.

2) Consumer cells at the interior core of the colony then utilize this galactose, and start to grow on top of the bottom layer of the producer cells, in a ring around the initial homogenous core region. Also, because of lactose depletion, the producer cells start to slow down, providing a window of opportunity for the consumer to reach the frontier.

3) But to keep up with the producer and not be completely cut off at the frontier, the consumer needs an extra boost in growth which it gets by simultaneously utilizing acetate along with galactose. Thus, when the producer eventually stops expanding radially, the consumer, which can still grow on the available galactose and acetate, starts to envelop the producer and produces the patterns.

Our cross-feeding agent-based simulations are still in the initial stage, one of the reasons being the cost of computation for the agent-based simulation of these large colonies in all the 3 dimensions, which is necessary to capture these patterns. Initial results (not shown) indicates that the model was able to capture the spatial heterogeneity in the z-direction for the producer and the consumer, indicating that we are on the right track.

Although in this study, our main aim was to address the dynamics of cross-feeding communities in colony growth, we discovered the formation of quite interesting patterns. Various unique pattern formation systems are found in nature, mostly on the macro scale, and although we are able to understand the biophysical nature of some of these patterns, engineering pattern formation using synthetic biology tools has largely remained elusive [34][35]. Understanding the factors which played a role in pattern formation in our system can help guide future construction of these self-organized systems in synthetic biology, thus reducing our knowledge gap about why and how these vast arrays of patterns form in nature and what are its implications.

Acknowledgements

Chapter 2, contains unpublished material coauthored with Kannan, Harish; Caglar, Tolga; Segota Igor; Zhang, Zhongge; Sun, Paul; Li, Bo and Hwa, Terence. The thesis author was a primary author of this chapter.

REFERENCES

1. Stewart, P. S., & Franklin, M. J. (2008). Physiological heterogeneity in biofilms. *Nature Reviews Microbiology*, *6*(3), 199-210.

2. Flemming, H. C., & Wingender, J. (2010). The biofilm matrix. *Nature reviews microbiology*, *8*(9), 623-633.

3. Warren, M. R., Sun, H., Yan, Y., Cremer, J., Li, B., & Hwa, T. (2019). Spatiotemporal establishment of dense bacterial colonies growing on hard agar. *Elife*, *8*, e41093.

4. Cole, J. A., Kohler, L., Hedhli, J., & Luthey-Schulten, Z. (2015). Spatially-resolved metabolic cooperativity within dense bacterial colonies. *BMC systems biology*, *9*(1), 1-17.

5. Pirt, S. J. (1967). A kinetic study of the mode of growth of surface colonies of bacteria and fungi. *Microbiology*, *47*(2), 181-197.

6. Wimpenny, J. W. (1979). The growth and form of bacterial colonies. *Microbiology*, *114*(2), 483-486.

7. Boyer, D., Mather, W., Mondragón-Palomino, O., Orozco-Fuentes, S., Danino, T., Hasty, J., & Tsimring, L. S. (2011). Buckling instability in ordered bacterial colonies. *Physical biology*, *8*(2), 026008.

8. Jayathilake, P. G., Gupta, P., Li, B., Madsen, C., Oyebamiji, O., González-Cabaleiro, R., Rushton, S., Bridgens, B., Swailes, D., Allen, B., McGough, A.S., Zuliani, P., Ofiteru, D. I., Wilkinson, D., Chen, J., & Curtis, T. (2017). A mechanistic Individual-based Model of microbial communities. *PloS one*, *12*(8), e0181965.

9. Baba, T., Ara, T., Hasegawa, M., Takai, Y., Okumura, Y., Baba, M., Datsenko, K.A., Tomita, M., Wanner, B.L. and & Mori, H. (2006). Construction of Escherichia coli K-12 in-frame, single-gene knockout mutants: the Keio collection. *Molecular systems biology*, *2*(1), 2006-0008.

10. Sauls, J. T., Li, D., & Jun, S. (2016). Adder and a coarse-grained approach to cell size homeostasis in bacteria. *Current opinion in cell biology*, *38*, 38-44.

11. Monod, J. (1949). The growth of bacterial cultures. *Annual review of microbiology*, *3*(1), 371-394

12. Pinhal, S., Ropers, D., Geiselmann, J., & De Jong, H. (2019). Acetate metabolism and the inhibition of bacterial growth by acetate. *Journal of bacteriology*, *201*(13), e00147-19.

13. Lin, Y. C., Cornell, W. C., Jo, J., Price-Whelan, A., & Dietrich, L. E. (2018). The Pseudomonas aeruginosa complement of lactate dehydrogenases enables use of d-and l-lactate and metabolic cross-feeding. *MBio*, *9*(5), e00961-18.

14. Díaz-Pascual, F., Lempp, M., Nosho, K., Jeckel, H., Jo, J. K., Neuhaus, K., Hartmann, R., Jelli, E., Hansen, M.F., Price-Whelan, A. and Dietrich, L.E., Link, H & Drescher, K. (2021). Spatial alanine metabolism determines local growth dynamics of Escherichia coli colonies. *Elife*, *10*, e70794.

15. Schink, S. J., Biselli, E., Ammar, C., & Gerland, U. (2019). Death rate of E. coli during starvation is set by maintenance cost and biomass recycling. *Cell systems*, *9*(1), 64-73.

16. Rooney, L. M., Amos, W. B., Hoskisson, P. A., & McConnell, G. (2020). Intra-colony channels in E. coli function as a nutrient uptake system. *The ISME journal*, *14*(10), 2461-2473.

17. Hallatschek, O., Hersen, P., Ramanathan, S., & Nelson, D. R. (2007). Genetic drift at expanding frontiers promotes gene segregation. *Proceedings of the National Academy of Sciences*, *104*(50), 19926-19930.

18. Kayser, J., Schreck, C. F., Yu, Q., Gralka, M., & Hallatschek, O. (2018). Emergence of evolutionary driving forces in pattern-forming microbial populations. *Philosophical Transactions of the Royal Society B: Biological Sciences*, *373*(1747), 20170106.

19. Kayser, J., Schreck, C. F., Gralka, M., Fusco, D., & Hallatschek, O. (2019). Collective motion conceals fitness differences in crowded cellular populations. *Nature ecology & evolution*, *3*(1), 125-134.

20. Goldschmidt, F., Regoes, R. R., & Johnson, D. R. (2018). Metabolite toxicity slows local diversity loss during expansion of a microbial cross-feeding community. *The ISME journal*, *12*(1), 136-144.

21. Goldschmidt, F., Regoes, R. R., & Johnson, D. R. (2017). Successive range expansion promotes diversity and accelerates evolution in spatially structured microbial populations. *The ISME journal*, *11*(9), 2112-2123.

22. Ciccarese, D., Micali, G., Borer, B., Ruan, C., Or, D., & Johnson, D. R. (2022). Rare and localized events stabilize microbial community composition and patterns of spatial self-organization in a fluctuating environment. *The ISME Journal*, 1-11.

23. Mitri, S., Clarke, E., & Foster, K. R. (2016). Resource limitation drives spatial organization in microbial groups. *The ISME journal*, *10*(6), 1471-1482.

24. Celik Ozgen, V., Kong, W., Blanchard, A. E., Liu, F., & Lu, T. (2018). Spatial interference scale as a determinant of microbial range expansion. *Science advances*, *4*(11), eaau0695.

25. Müller, M. J., Neugeboren, B. I., Nelson, D. R., & Murray, A. W. (2014). Genetic drift opposes mutualism during spatial population expansion. *Proceedings of the National Academy of Sciences*, *111*(3), 1037-1042.

26. Van Dyken, J. D., Müller, M. J., Mack, K. M., & Desai, M. M. (2013). Spatial population expansion promotes the evolution of cooperation in an experimental prisoner's dilemma. *Current Biology*, *23*(10), 919-923.

27. Amarnath, K., Narla, A. V., Pontrelli, S., Dong, J., Caglar, T., Taylor, B. R., Schwartzman, J., Sauer, U., Cordero, O. X. & Hwa, T. (2021). Stress-induced cross-feeding of internal metabolites provides a dynamic mechanism of microbial cooperation. *bioRxiv*.

28. Morris, B. E., Henneberger, R., Huber, H., & Moissl-Eichinger, C. (2013). Microbial syntrophy: interaction for the common good. *FEMS microbiology reviews*, *37*(3), 384-406.

29. Cremer, J., Segota, I., Yang, C. Y., Arnoldini, M., Sauls, J. T., Zhang, Z., Gutierrez, E., Groisman, A. & Hwa, T. (2016). Effect of flow and peristaltic mixing on bacterial growth in a gut-like channel. *Proceedings of the National Academy of Sciences*, *113*(41), 11414-11419.

30. Owens, J. D., & Legan, J. D. (1987). Determination of the Monod substrate saturation constant for microbial growth. *FEMS Microbiology Reviews*, *3*(4), 419-432.

31. Lendenmann, U., Snozzi, M., & Egli, T. (1999). Growth kinetics of Escherichia coli with galactose and several other sugars in carbon-limited chemostat culture. *Canadian journal of microbiology*, *46*(1), 72-80.

32. Balakrishnan, R., de Silva, R. T., Hwa, T., & Cremer, J. (2021). Suboptimal resource allocation in changing environments constrains response and growth in bacteria. *Molecular systems biology*, *17*(12), e10597.

33. Okano, H., Hermsen, R., & Hwa, T. (2021). Hierarchical and simultaneous utilization of carbon substrates: mechanistic insights, physiological roles, and ecological consequences. *Current Opinion in Microbiology*, *63*, 172-178.

34. Luo, N., Wang, S., Lu, J., Ouyang, X., & You, L. (2021). Collective colony growth is optimized by branching pattern formation in Pseudomonas aeruginosa. *Molecular systems biology*, *17*(4), e10089.

35. Liu, C., Fu, X., Liu, L., Ren, X., Chau, C. K., Li, S., Xiang, L., Zeng, H., Chen, G., Tang, L.H., Lenz, Peter., Cui, X., Huang, W., Hwa, T., Huang, J.D. (2011). Sequential establishment of stripe patterns in an expanding cell population. *Science*, *334*(6053), 238-241.